ISTANBUL TECHNICAL UNIVERSITY ★ GRADUATE SCHOOL OF SCIENCE ENGINEERING AND TECHNOLOGY

PROCESSING AND ANALYSIS OF ZIRCONIA BASED REFRACTORIES

M.Sc. THESIS

Sina SADIGH AKBARI

Department of Metallurgical and Materials Engineering

Materials Engineering Programme

MAY 2015

ISTANBUL TECHNICAL UNIVERSITY ★ GRADUATE SCHOOL OF SCIENCE ENGINEERING AND TECHNOLOGY

PROCESSING AND ANALYSIS OF ZIRCONIA BASED REFRACTORIES

M.Sc. THESIS

Sina SADIGH AKBARI
(506131430)

Department of Metallurgical and Materilas Engineering

Materials Engineering Programme

Thesis Advisor: Prof. Dr. Serdar OZGEN

MAY 2015

İSTANBUL TEKNİK ÜNİVERSİTESİ ★ FEN BİLİMLERİ ENSTİTÜSÜ

ZİRKONYA ESASLI REFRAKTERLERİN PROSES VE ANALİZLERİ

YÜKSEK LİSANS TEZİ

Sina SADİGH AKBARİ
(506131430)

Metalurji ve Malzeme Mühendisliği Anabilim Dalı

Malzeme Mühendisliği Programı

Tez Danışmanı: Prof. Dr. Sedar ÖZGEN

MAYIS 2015

Sina SADIGH AKBARI, a **M.Sc.** student of ITU **Graduate School of Science and Engineering** student ID 506131430, successfully defended the **thesis** entitled "**PROCESSING AND ANALYSIS OF ZIRCONIA BASED REFRACTORIES**", which he prepared after fulfilling the requirements specified in the associated legislations, before the jury whose signatures are below.

Thesis Advisor :   **Prof. Dr. Serdar OZGEN**   ....
                                        Istanbul Technical University

Jury Members :   **Prof. Dr. Lutfi OVECOGLU**   ....
                                    Istanbul Technical University

                                    Prof. Dr. Suat YILMAZ   ....
                                    Istanbul University

Date of Submission : 04 May 2015
Date of Defense :   29 May 2015

To my parents,

FOREWORD

I would like to express my deepest gratitude to my supervisor, Prof. Dr. Serdar Ozgen for giving me an opportunity to work in this project, for his guidance, support and encourgment during the entire course of this work.

My sincere thanks to Prof. Dr. Lutfi Ovecoglu for the immense support, friendly coopereation and constructive discussion.

Special thanks to Dr. Cagatay Durmus for help guidence and Metamin A.S. for providing raw materials and their support during this project.

I would also like to thank all my friends and colleagues and all staff and members at the PML for providing the supportive working environment, especially to my laboratory colleagues Emre Tekoglu.

Finally, I would like to thank my parents, for all his love and supports.

May 2015   Sina Sadigh Akbari
                                                        (Materials Engineer)

TABLE OF CONTENTS

ABBREVIATIONS

ZrO₂   **:** Zirconium dioxide
MgO   **:** Magnesium oxide
TiO₂   **:** Titanium dioxide
Si₃N₄   **:** Silicon nitride
SiC   **:** Silicon carbide
m   **:** Monoclinic zirconia
c   **:** Cubic zirconia
t   **:** Tetragonal zirconia
XRD   **:** X-ray diffraction
SEM   **:** Scaning electron microscopy
PSZ   **:** Partially stabilized zirconia
TZP   **:** Tetragonal zirconia polycrystal
FSZ   **:** Fully stabilized zirconia
GPa   **:** Gigapascal
MPa   **:** Megapascal
K$_{IC}$ **:** Fracture toughness
PVA   **:** Polyvinyl alcohol
ASTM   **:** American Society for Testing and Materials
o   **:** Orthorhombic zirconia
ss   **:** Solid solution

LIST OF TABLES

LIST OF FIGURES

PROCESSING AND ANALYSIS OF ZIRCONIA BASED REFRACTORIES

SUMMARY

During recent years, significant progress has been done in the development of engineering ceramic materials. A new generation of ceramics has been developed which are expected to find wide use in applications at high temperatures.

Among these materials, zirconia (ZrO_2) is an attractive candidate for high temperature applications because of its high melting point and excellent corrosion resistance. Unfortunately the tetragonal to monoclinic phase change is a martensitic transformation with a volume increase of about 3–5% so that if a component is cooled through the transformation temperature it becomes heavily microcracked, decreasing the Young modulus and the strength, although it increases the resistance to catastrophic failure. In this study some dopants were added to both monoclinic and tetragonal stabilized zirconia in order to mechanical properties improvement.

Raw materials based on zirconia were studied to synthesize refractory material for metallurgical applications. Fused MgO stabilised Zirconia and chemicaly precipitated monoclinic zirconia were supplied and characterized using XRD, SEM and some mechanical tests.

Fused MgO stabilised Zirconia powders with addtion of TiO_2, SiC and Si_3N_4 were subjected to various test to determine the suitable doppant content for improving mechanical properties. Various mixtures with different composition were prepared in dry form. Particle size distribution is checked according to Dinger&Funk theory. Samples were pressed and sintered in air, nitrogen and argon atmosphere.

The effect of TiO_2, SiC and Si_3N_4 addition on the mechanical properties of monoclinic zirconia and tetragonal stabilized zirconia during the sintering and in-situ stabilization have been investigated. The composition of zirconia and MgO was prepared with 0, 5, 10, 15% TiO_2, Si_3N_4 or SiC addition by weight percent respectively. MgO content was kept unchanged. The powder with PVA as a binder was mixed and reduced in size by wet milling. Milling procedure was kept same in order not to change grain size then the powder was shaped by press with the same procedure as before. The specimens were then sintered at 1400°C and 1600°C with the same procedure applied before stabilization. After sintering;

-     XRD
-     SEM
-     Density and apparent porosity
-     Hardness
-     Bending strength
-     Fracture toughness

were studied.

In zirconia containing Si_3N_4 specimens, monoclinic phase was decreased and tetragonal, cubic and zirconium oxide nitride phase were formed (β:$Zr_7O_8N_4$). Decreasing densification specimens can be related to low powder density of silicon nitride (3.44 g/cm^3). Flexural strength, hardness and fracture toughness values are increased by increasing Si_3N_4 content.

XRD analysis revealed $Mg_2Zr_5O_{12}$ structure and tetragonal phase formed only in 5 wt% TiO_2 containing specimens. Doping TiO_2 to zirconia was destabilized zirconia and titanium dioxide reacted with MgO. Density of all samples decreased with increasing of TiO_2. This decreased density can be due to the grain growth and increasing amount of intergranular porosity.

Hardness was reduced with increasing TiO_2 content, and it can be explained by increasing amount of porosities. Zirconia containing 5 wt % TiO_2 was showed relatively high flexural strength and fracture toughness at lower sintering temperature.

Doping TiO_2 and sintering at 1400°C without ageing process presented better mechanical properties for both monoclinic and tetragonal powder. Also increasing TiO_2 over 5 wt% changed microstructure, where decreased hardness, flexural strength and fracture toughness values.

In the case of silicon carbide specimens, according to X-ray diffraction patterns and strength values sintering temperature was not enough high and specimens were not densificated.

ZİRKONYA ESASLI REFRAKRELERİN PROSES VE ANALİZLERİ

ÖZET

Zirkonya esaslı refrakter seramikler kendine özgü mikroyapısal ve mekanik özellikler göstermesi sayesinde; ergime sıcaklığının yüksek olması, termal şoka dayanıklı olması, korozyon ve aşınmaya karşı dayanıklı olması, asidik kimyasal maddelere, cürufa ve cama karşı direncinin yüksek olması, kırılma indisinin yüksek olması gibi özellikler gösterirler. Bu özellikleri zirkonyanın yüksek sıcaklık malzemesi olarak refrakter uygulamarında, estetik ve işlevsel bir malzeme olarak termal bariyer kaplama, yakıt pili ve biyouyumlu olarak biyomalzemeler gibi birçok uygulama alanında kullanılmasını sağlamaktadır. Bununla birlikte, son yıllarda zirkonya esaslı seramiklerin dönüşüm toklaşma mekanizması gibi özelliklerinin geliştirilmesi ile bu seramiklerin mühendislik seramikleri uygulamalarında kullanımı artmıştır.

Saf zirkonya, Monoklinik (m), tetragonal (t) ve kübik (c) faz olmak üzere üç adet kristal yapıya sahiptir. ZrO_2 yapısında hangi polimorfun bulunacağı, sıcaklığa ve basınca bağlıdır. Atmosferik basınçta, m-faz 1170°C'ye kadar kararlıdır. Bu sıcaklıkta m-faz, t-faza dönüşür ve oluşan t-faz, 2300°C'ye kadar kararlıdır. 2300°C'den ergime sıcaklığı olan 2700°C'ye kadar ise ZrO_2, c-faz şeklinde bulunur. Bu üç faza ilaveten, yüksek sıcaklık ve basınç altında ortorombik (o) fazı da oluşmaktadır. Bu polimorfik dönüşümler sırasında zirkonya hacimsel değişikliğe uğrayarak özellikle termal şok özelliklerinin olumsuz yönde etkilenmesi nedeniyle yüksek sıcaklık uygulamalarında kullanımını kısıtlanmaktadır. Bu nedenle stabilize edici oksitlerin yardımıyla zirkonyanın oda sıcaklığında tetragonal+kübik faz ya da kübik fazında kararlı halde bulunması sağlanır.

Yaygın olarak stabilize edici oksit olarak MgO, CaO ve Y_2O_3 kullanılmaktadır. Bu oksitlerden hangisinin ve hangi miktarlarda seçileceği çalışılmak istenen ve üründen beklenen özelliklere göre değişiklik gösterebilmektedir. Yine aynı şekilde kısmen stabilizasyon bölgesinde ya da tamamen stabilize zirkonya bölgesinde çalışılacağı ilgili faz diyagramlarından seçilerek kullanılmak istenilen stabilize edici oksit miktarı belirlenir.

Zirkonya esaslı refrakterler oda sıcaklığında sağladığı özellikleri yüksek sıcaklıklara kadar muhafaza edebilirler. Bu özellikleri zirkonya esaslı refrakterleri yüksek sıcaklık fırınlarında kullanışlı hale getirmektedir. Genellikle cam ergitme fırınlarında, gösterdiği asidik karakter ve yüksek sıcaklıklarda sağladığı mukavemet sayesinde zirkon esaslı tuğlalar yaygın olarak kullanılmaktadırlar. Ayrıca yüksek aşınma dirençleri, stabilize edilmiş zirkonyanın yüksek termal şok direnci ve çelik ile ıslanmaması sayesinde zirkonyanın çelik üretimi için kullanılan tandiş nozüllerinde kullanımını yaygın olarak sağlamaktadır. Zirkonya esaslı refrakterler diğer refrakter malzemelere oranla daha düşük termal iletkenliğe sahiptir, bu nedenle yüksek sıcaklıkta iyi bir izolasyon refrakter malzemesi olarak da kullanılabilmektedirler.

Bu çalışmada, yüksek saflıktaki monoklinik zirkonya tozuna stablize edici oksit olarak MgO ve katkı maddesi olarak TiO_2, Si_3N_4 ve SiC eklenmiş ve sonrasında yapısal ve mekanik özellikleri incelenmiştir. Kullanılan oksit miktarı, ilgili faz diyagramından kısmen stabilize zirkonya bölgesine denk gelen aralıklardan seçilmiştir. Numunelerin fiziksel ve kimyasal özellikleri X ışınları difraksiyon analizi, yoğunluk ve gözeneklilik ölçümü, sertlik testi, eğme testi, kırılma tokluğu testi, ve SEM analizleri ile belirlenmiştir.

Monoklinik zirkonya tozuna stablize edici olarak %3.12 ağırlık MgO ve katkıcı olarak %0-5-10-15 ağırlık aralıklarında TiO_2, Si_3N_4 veya SiC eklenmiştir. Ayrıca TiO_2 katkılı numunede tetragonal stablize edilmiş zirkonya tozu da başlangıç maddesi olarak kullanılmıştır.

Belirtilen oranlarında hazırlanan kompozisyonlar bilyeli değirmende, etanol alkol ortamında, Y-SZP bilyeler yardımıyla ve %3 bağlayıcı (PVA) katkısıyla dört saat öğütülmüşlerdir. Etüvde 120°C'de etanol ortamından uzaklaştırılan kompozisyonlar ≈22MPa basınç altında el presinde şekillendirilmişlerdir. Şekillendirilen tüm numuneler 2°C/dak ısıtma ve soğutma hızıyla 600°C'de bağlayıcı giderme işlemi uygulanmıştır. Bağlayıcı giderme işlemi sonrası numunelere ısıl işlem uygulanmıştır. Si_3N_4 ve SiC katkılı numuneler 5°C/dak ısıtma ve soğutma hızıyla 1600°C'de 2 saat bekletilmiş. Bu çalışmada TiO_2 katkılı numunelere iki farklı sinterleme sıcaklığı uygulanmıştır. 1) Numuneler 5°C/dak hızında 1300°C'ye ısıtılmış hemen akabinde 1600 °C sıcaklığa 2°C/dak hızında çıkartılmıştır ve bu sıcaklıkta bütün numuneler 5 saat bekletildikten sonra yaşlandırma sıcaklığına 5°C/dak hızında soğutulmuştur ve yaşlandırma sıcaklığında 4 saat bekletilmiştir, 2) numuneler 5°C/dak ısıtma ve soğutma hızıyla 1600°C'de 2 saat bekletilmiş.

Isıl işlem sonucu elde edilen numunelere X-ışınları difraksiyon analizi, yoğunluk ve gözeneklilik ölçümü, sertlik testi, eğme testi, kırılma tokluğu testi, ve SEM analizleri uygulanmıştır ve bulunan sonuçlar birbiri ile karşılaştırılmıştır.

- Isıl işlem sonucu elde edilen numunelere X-ışınları difraksiyon analizi sonucunda katkı maddelerinin oranı arttıkça monoklik fazının fazının yoğunlaştığı gözlenlenmiştir. Bunun nedeni katkı maddelerinin MgO ile reaksiyona girmesidir.

- Si_3N_4 katkı miktarı arttıkça sertlik, kırılma tokluğu ve eğme testi değeri artmıştır. Ayrıca zirkonyom oksit nitrit fazının oluşmasına ve çoğalmasına sebep olur.

- TiO_2 katkı miktarı ağırlık yüzde beşe kadar mekanik özellikleri gelişmiştir ama ondan sonra katkı miktarının artması mekanik özellikleri kötü yönde etkilemiştir. Ayrıca bu numunelerde düşük sıcaklıklarda sinterlenmiş numunelerin mekanik özellikleri yüksek sıcaklıklarda sinterlenmiş numunelerlen daha iyi olduğu görülmüştür. Bunun nedeni oalrak SEM sonuçlarına göre bu numunelerde TiO_2 oranı arttıkça tane boyutunun büyüdüğü görülmüştür.

- SiC katkı maddesi ergime sıcaklığı yüksek olduğundan dolayı numunelerin sinterlenmesini önlediği gözlenlenmiştir.

1. INTRODUCTION

Zirconia (ZrO_2) is an extremely versatile ceramic, which is an attractive candidate for oxygen pumps and sensors, fuel cells, thermal barrier coatings, and other high-temperature applications. All these applications use of the electrical, thermal, and mechanical properties of zirconia [1].

Pure ZrO_2 exists in three different crystal structures, monoclinic, tetragonal and cubic. These phases can be obtained depending on temperature and compositional ranges under equilibrium conditions. The tetragonal to monoclinic phase transition is a martensitic transformation which associated with a volume change of about 3–5% so that if a component is cooled through the transformation temperature it becomes heavily microcracked, decreasing the strength [2, 3].

The addition of varying amounts of the stabilizing oxide, particularly MgO, CaO and Y_2O_3, has been modified the phase transition and developed novel and innovative ceramic materials which have brought about considerable thechnologic change. This is useful in applications like refractories where it is this latter property rather than a high strength which is most required [3, 4].

ZrO_2-based systems have been developed commercially, depending on the type and amount of doping. Partially stabilized zirconia (PSZ) has a lower content of stabilizer, such that the cubic cannot be the only phase, and tetragonal and monoclinic phases also exists. The relative amounts of the tetragonal and cubic phases in the mixture can be easily changed by choosing an appropriate amount of doping [5].

Transformation toughening of ZrO_2 was first reported in a paper entitled "Ceramic Steel" by Garvie, Hannink, and Pascoe in 1975 [6]. This title might be chosen to emphasize the features that ZrO_2-based alloys have in common with alloys of iron. ZrO_2 has athermal expansion coefficient and elastic modulus similar to those of steel. Zirconia has several allotropes which can be alloyed to achieve a variety of microstructures and resulting properties [7].

The objective of this thesis was to study developing the mechanical properties of both monoclinic and tetragonal stabilized zirconia by use of dopants. Specimens were prepared with addition of TiO_2, Si_3N_4 or SiC to zirconia powders which sintered at different temperatures. Phase analysis and microstructure investigation were done by X-ray diffraction (XRD) and scanning electron microscopy (SEM), also three-point bending test, Vicker's hardness and fracture toughness values were used to compare difference of mechanical properties between specimens.

2. LITERATURE REVIEW

2.1 Zirconia

Zirconium is a chemical element with atomic number 40. The name of "Zirconium" comes from Persian word "Zargon", meaning "golden in color". Zirconium dioxide was discovered by Martin Heinrich Klaproth, who is a German chemist, while working with the composition of the $ZrSiO_4$ in 1789 [8].

The element Zirconium is found in a igneous rocks such as schists, gnesis, syenite, and granite [4]. The zirconium compounds are obtained mainly as the free oxide baddeleyite with small amount of hafnium oxide present and as zircon beach sand with silica ($ZrO_2.SiO_2$) [3].

Zircon, zirconium orthosilicate, is the large secondary deposits in beach sands because of a combination of weathering and natural concentration due to the its high density ($\rho = 4.6$). It is found in most igneous rock and some metaphormic rocks as a small crystals and grains. Therefore, it is the most common and widely distributed of the commercial minerals. Important commercial deposits are mined in Australia, India, South Africa and U.S.A., the greatest amount is used directly in the manufacture of refractories. However because of its widespread occurrence and suitable price, zircon is also used for zirconium chemicals, which purity of ziconia is required for their process [4].

Baddeleyite, ZrO_2, is less widely distributed than zircon and is usually found associated with 1-1.5% each of silica and iron oxide [4]. Large deposits of baddeleyite (monoclinic zirconia) are present in Brazil (Sao Paulo and Minas Gereas) [9], also recently South Africa (Palabora) has become the major source of this mineral where it products as a by-product in the concentration of copper and uranium minerals. Baddeleyite which associated with alumina, is used for the production of grinding wheels in the abrasive manufacturing industry and also finds application as a refractory. The source of minerals and their chemical compositions are shown in Table 2.1 [4].

Table 2.1 : Raw materials for the production of zircon and zirconia [4].

Chemical Analysis	Australian Zircon	S. African Foskor	Baddeleyite Foskor
Zirconia %	66.90	96	> 99
Silica %	32.60	1.5	< 0.5
Titanium Oxide %	0.12	1	< 0.3
Ferric Oxide %	0.04	1	< 0.05
Alumina %	0.43		
Lime %			
Magnesia %	0.03		
Phosphoric anhydride %	0.007	0.2	< 0.03

2.2 Crystal Structure and Properties

Pure zirconia can exist in three crystal structures, i.e., monoclinic, tetragonal and cubic, which have same chemical composition but different atomic arrangement. These phases can be obtained depending on temperature and compositional ranges under equilibrium conditions [2, 9]:

$$\text{monoclinic} \xleftrightarrow{1170\,°C} \text{tetragonal} \xleftrightarrow{2370\,°C} \text{cubic} \xleftrightarrow{2680\,°C} \text{liquid}$$
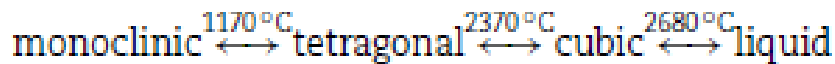
Figure 2.1 : Zirconia phase transformation in terms of temperature [9].

A monoclinic structure stable at lower temperatures until 1170°C , a tetragonal form stable at terminate temperatures (1170°C-2370°C), a cubic form exist at the highest temperatures, between the melting point (2680°C) and 2370°C [3].
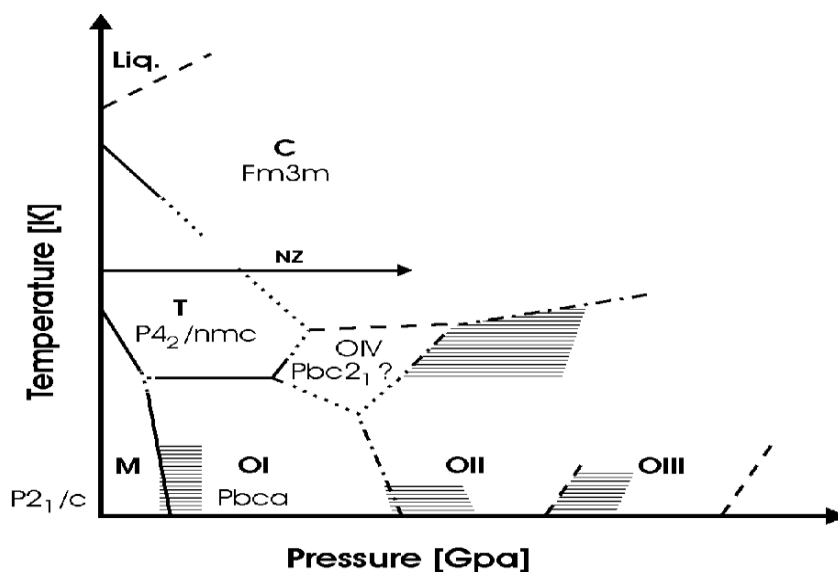
Figure 2.2 : Pressure-temperature phase diagram of zirconia [5].

Table 2.2 : Crystallographic data of zirconia [10].

Modification	Monoclinic Zirconia	Tetragonal Zirconia	Cubic Zirconia
Space group	$P2_1/c$	$P4_2/nmc$	$Fm3m$
Lattice parameters (pm)	a = 516 b = 519 c = 530 $\beta = 98.9°$	a = 509 c = 518	a = 512
Density (g/cm³)	5.83	6.10	6.09

2.2.1 Monoclinic ZrO_2

The monoclinic (baddeleyite) structure is the stable form of ZrO_2 at room temperature, which Zr^{4+} has the coordination number of 7. This unusual structure is a result of the non-planar arrangement of the oxygen ions, where four oxygen atoms (O_{II}) form with the central zirconium atom an almost symmetrical tetrahedral arrangement; there remaining oxygen atoms (O_I) are strongly disordered (Figure 2.3a) [5, 10].

Because of this reason there is a tendency for twining in baddeleyite. Since the oxygen ions are out of their symmetric position, small contortions of the lattice are expected [5]. The twin plane (001) is composed of O_{II} atoms that are rather mobile and can easily be moved out of their equilibrium positions. In the projection onto the (010) plane (Figure 2.3b), the boundary of the twin plane (001) is shown as the dotted line [10].
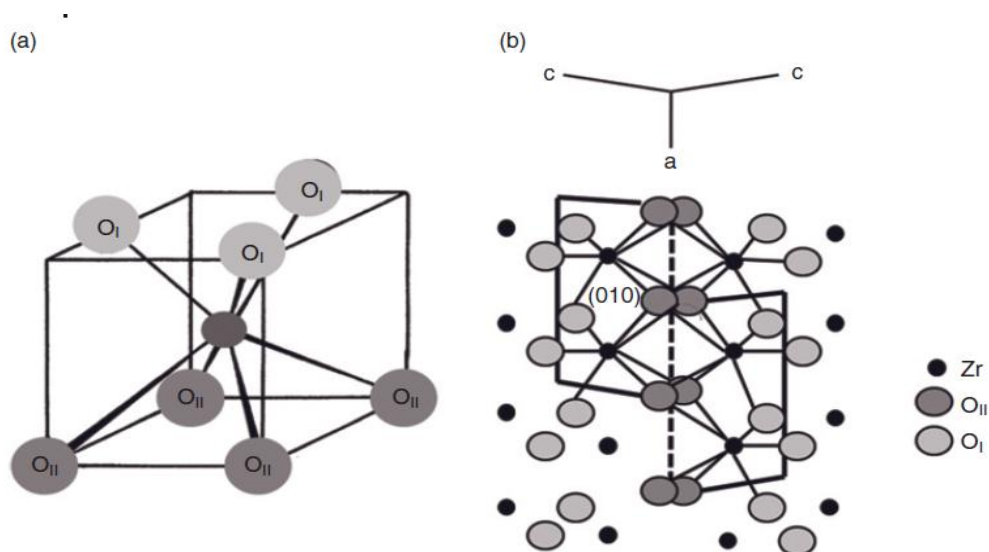
Figure 2.3 : Structure of monoclinic zirconia. (a) Idealized ZrO_7 polyhedron, showing the two types of oxygen (O_I and O_{II}); (b) Projection onto the (010) plane, showing the plane of twinnig (dotted line) [10].

2.2.2 Tetragonal zirconia

The monoclinic structure will transform into a distorted tetragonal fluorite structure with a higher density. This reversible transformation occurs above 1170°C and tetragonal form stables below 2370°C [5]. In this phase, Zr^{4+} atoms are coordinated octahedrally to the oxygen atoms, which are no longer equidistant. Instead, four are approximately 15% closer to the Zr atoms than the other four oxygen atoms [11].

The tetragonal phase can be transform into the monoclinic phase during cooling. The composition (fraction, size and distribution) of the tetagonal phase controls the 'zirconia based ceramics' properties and microstructure [5].
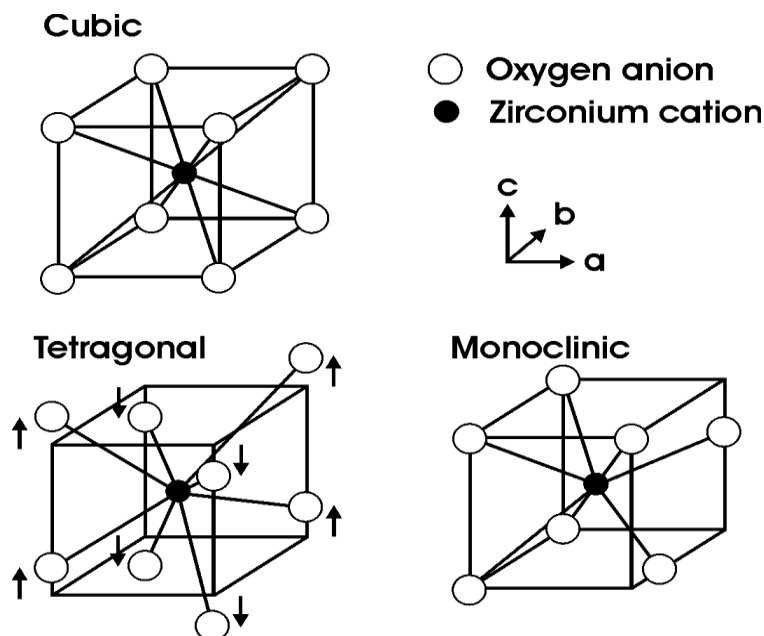
Figure 2.4 : Crystal structure of cubic, tetragonal and monoclinic ZrO_2 [5].

2.2.3 Cubic zirconia

The cubic phase, which is stable from 2370°C to the melting point, has the face-centered cubic (f.c.c) fluorite-type structure with each Zr^{4+} atom octahedrally coordinated with eight oxygen atoms, all at an equal distance. Oxygen atoms are tetrahedrally coordinated to four equidistant Zr atoms [11].

2.3 Zirconia Phase Transformation

Examined upon cooling, these lattice transformations are athermal, diffusionless (i.e involving only coordinated shifts in lattice positions versus transport of atoms) and involving a shape deformation, which the term "martensitic" used to describe these

types of transformation. Furthermore volume changes associated with these transformations are enough to make the pure materials unstable: cubic $\rightarrow$ tetragonal is 2.3% and tetragonal $\rightarrow$ monoclinic is 4.5%. In both cases, the driving force for the transformation is so high (free energy of the t-phase G_t >> the free energy of the c-phase G_c in the former, and the free energy of the m-phase G_m >> G_t in the latter transformation) [11, 12].

Being about 1972, ceramic engineering community was discovering that the tetragonal or even cubic form could be retained metastably at room temperatures by alloying zirconia with other cubic and low valance oxides, such as CaO, MgO, La_2O_3, GeO_2 and Y_2O_3, thus the strained monoclinic phase was disfavored and favored more symmetric cubic and tetragonal lattice structures. It becomes now clear why such oxides have been termed "stabilizer" [9, 12].

2.3.1 Monoclinic-tetragonal transformation

In the pure undoped zirconia, tetragonal-monoclinic transformation during cooling is martensitic transformation, it occurs with a large temperature hysteresis (around 200°C for undoped zirconia) and associated with volume change (4-5%) [13]. The hysteresis width is controlled by processing history of the materials, the amount and type of stabilizing ions, and also by grain size [10].

This martensitic and reversible transformation of the metastable tetragonal to the monoclinic is induced either during thermal cooling or by external stress application. The stress-induced martensitic transformation of tetragonal ZrO_2 enhances toughness, and this phenomenon is known as transformation toughening [14].

The t$\rightarrow$m transformation typically occurs in two major step, in the first step, the transition from tetragonal to monoclinic takes place by shear displacement of zirconium ions, and in the second step oxygen ions migrate to their respective sites in the monoclinic symmetry. The reverse transition of the lattice structure from monoclinic symmetry to tetragonal symmetry and the migration of the Zr^{+4} and O^{-2} ions to their respective positions are controlled by the diffusional displacements of the respective ions [14].

Garvie et al. for the first time realized that the phase transformation of zirconia can be used in enhancing the mechanical properties of ceramic [6], and subsequently developed the concept of transformation toughening. The volume change during

transformation and shear strain can be opposed the opening of the crack, therefore the resistance of the ceramic to crack propagation increases [15].

The transformation was shown to be dependent on the particle size, decreasing particle size of zirconia powder was reduced transformation temperature. Andersson and Gupta have researched on the effect of particle size on phase stability, there is now a consensus of opinion agreeing that nucleation of the martensitic platelets is the significant factor in the transformation. Other factors, such as the size, charge and amount of stabiliser cations, the grain shape, temperature, oxygen vacancy concentration and residual stress can influence on transformation [4, 13].
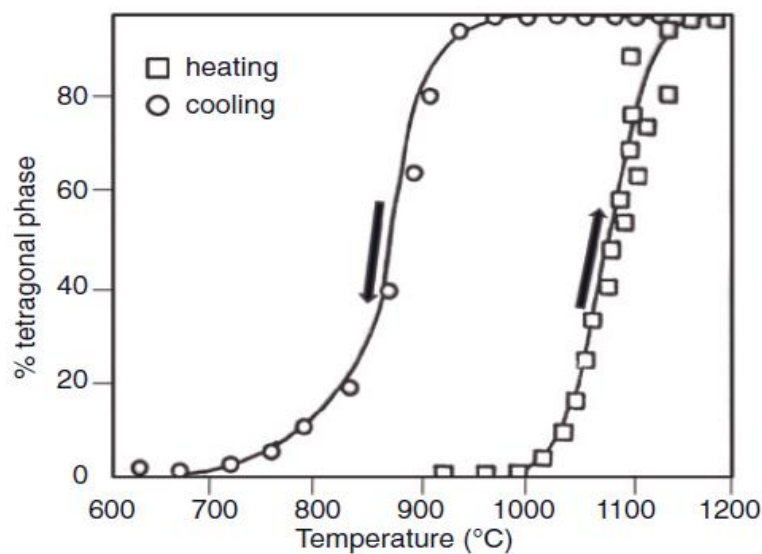
Figure 2.5 : The monoclinic-tetragonal transformation on heating and cooling of pure zirconia through the transformation temperature [4].

2.3.2 Tetragonal-cubic transformation

Since cubic-tetragonal phase transition in pure zirconia takes place at very high temperature, little is known about the nature of that. This transition not only is of intrinsic interest, but is also important because it has been suggested that the reverse transition [16]. Cubic to tetragonal transformation, which occurs at approximately 2370°C, has high driving force. It is thermodynamically impossible to retain either cubic or tetragonal phase at room temperature, even with rapid quenching [11].

2.4 Stabilization of Zirconia

Tetragonal-monoclinic phase transition associates with large volume changes, which have unsuitable effect on the pure materials, has received much attention from

8

scientists, technologists and users. Researchs have indicated some general criteria for selecting stabilizing oxides. These four criteria are: 1) the cation radii should be close to that of Zr^{+4} (0.084 nm) to minimize lattice distortions which can lead to high shear stresses and spontaneous transformations; 2) the cation should have a stable +2 or +3 state, which, when added to the ZrO_2, will produce oxygen vacancies; 3) the oxide crystal structure should be cubic or tetragonal, depending on the ZrO_2 phase to be stabilized; and 4) the oxide should have some degree of solubility in ZrO_2, with a higher solubility preferred. Based on these rules the addition of alkaline earth metal oxides or transition metal oxide like CaO, MgO, La_2O_3 or Y_2O_3 disfavor the monoclinic phase, stabilizing more symmetric structures with cubic and tetragonal symmetry . The amount of dopant required for the stabilization depends upon the nature of the dopant and, most importantly, upon the method of preparation [11, 17, 18].

In c∗ and t∗ (t∗ : metastable tetragonal, c∗ :metastable cubic) phases dopant ions substitute on Zr^{4+} sites and have fraction of oxygen sites vacant to retain charge neutrality , through which the electric charge can be transported in the form of ions [5, 12].

The simultaneous presence of dopant cations and oxygen vacancies in large concentration means that the local atomic environments in the stabilized material are very different from the corresponding stoichiometric (t and c) phases. Despite the analogy in the sequences m–t–c and m–t∗–c∗, there is no clear picture of the microscopic mechanisms of stabilization to parallel our understanding of the pure material, the most relevant issue concerns the respective roles of impurity cations and of oxygen vacancies [19].

2.4.1 Fully stabilized zirconia (FSZ)

Zirconia based ceramics have different types, which depend on the type and amount of doping. Highly doped, fully stabilized zirconia (FSZ) is a solid solution, which can no longer be transformed to any other phase. Development of tetragonal and cubic phases are controlled by the solubility of the dopant and diameter of the atom. However, in practical applications, the dopants are limited to rare earth elements and their substitutes (e.g. yttrium) [5].

2.4.2 Partially stabilized zirconia (PSZ)

These types of zirconia ceramic are the most widely investigated, commercially important, microstructurally complex, and in the case of Mg-doped some of the toughest ceramic. Their microstructure contains stabilized cubic which makes the matrix and tetragonal phase intra-granular precipitates exist within it. MgO, CaO, La_2O_3 and Y_2O_3 are used for stabilization, in concentrations lower than that required for fully cubic stabilized zirconia [12]. In fact, partially stabilized zirconia is a mixture of the cubic and tetragonal/monoclinic phases that can be prepared by heat treatment of the cubic phase [15].

Precipitates form on a nanometer scale with lenticular morphology (approximately 200nm diameter and 75nm thick), also they are fully coherent parallel to the three cubic axis (Figure 2.6). Following sintering or solution annealing in the cubic solid solution single-phase field (>1850°C), precipitates can be nucleated and grown at lower temperature (approximately 1100°C) within the two-phase tetragonal solid solution plus cubic solid solution phase field by a process named aging. Aging optimized both precipitates size and phase stability [12].

The aim of cooling is to uniformly distribute the tetragonal grains, retain as many of the precipitated grains in the tetragonal phase at room temperature as possible, and avoid the precipitation of the tetragonal grain boundaries, which can lead to the spontaneous transformation to monoclinic grains [11]. Metastability can be lost when precipitates are too small (they will not transform) and when they are too large transform to monoclinic phase with twinning and microcraking [12].
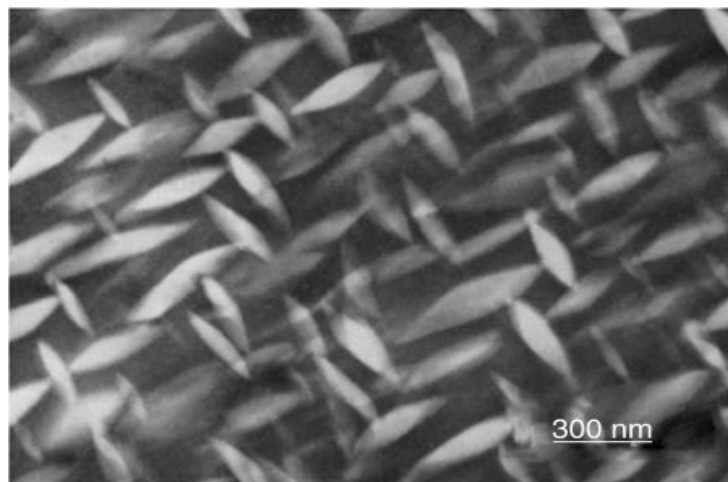
Figure 2.6 : Lenticular-shaped tetragonal zirconia precipitates in magnesia-partially stabilized zirconia [10].

The K_{IC} (fracture toughness) values of PSZ are very much higher than those of other engineering ceramics, varying between 7 (CaO-PSZ with 3.3 mass% CaO), 9 (MgO-PSZ with 3.4 mass% MgO), 10 (Y_2O_3-PSZ with 8 mass% Y_2O_3) MNm$^{-3/2}$. Because of this feature, one of the first reports which describing the mechanism of tansformation toughening of zirconia to refer to "ceramic steel" (Garvie et al., 1975). The thermal shock resistance of PSZ is good, due to the existence of abundance monoclinic phase [10, 20].

Table 2.3 : Ca-PSZ, Y-PSZ, Mg-PSZ mechanical properties [7].

Properties	Y_2O_3 PSZ zirconia	CaO PSZ zirconia	MgO PSZ zirconia
Amount (%)	5-10	3-4.5	2.5-3.6
Young's Modulus (GPa)	180-220	200-220	170-210
Bending Strength (MPa)	650-1000	400-650	440-720
Fracture toughness (MPa.m$^{1/2}$)	6-8	6-12	6-20
Hardness (GPa)	8-12	14-17	10-14

2.4.3 Tetragonal zirconia polycrystal (TZP)

The toughening effect in zirconia is increased linearly with the increasing amount of retained tetragonal phase. The logical consequence of this process is the development of ceramics that wholly tetragonal. This achievement was first accomplished by Rieth, and later by Gupta et al. [21], who prepared the ceramic by sintering yttria in the temperature range 1400-1500°C. Moreover, the critical grain size for the t→m transformation was found to depend on the amount of stabilizing aids, this being about 0.2 μm for 2 mol% Y_2O_3 and 1.0 μm for 3 mol% Y_2O_3, as well as on the presence or absence of mechanical constraints. The typical properties of TZP are summarized in Table 2.4 [15].

These type of ceramics are essentially homogeneous and their properties are function of grain size, in which grain size controls M_s temperature and the ease of transformation and hence the toughness effect. If grains become much smaller than the critical size, the toughness increment decreases because of over-stabilization of the grains which eliminate the t → m transformation upon introduction of a crack [12].

Table 2.4 : Typical properties of TZP [15].

Properties	Y-TZP
Melting point (°C)	2720
Bulk density (g.cm^{-3})	6.05
Young's Modulus (GPa)	140-200
Bending Strength (MPa)	900-1300
Fracture toughness (MPa.m$^{1/2}$)	5.5-11
Hardness (GPa)	14

This grain size effect itself is controlled by the type of dopant and the dopant concentration that are essentially determining the degree of tetragonality. Based on tetragonality, at similar grain size and dopant concentration yttrium appears to be stronger stabilizer [12].

Commercial TZP ceramics have a different microstructure from ideal form. They contain amorphous grain boundary phases and a significant amount of the cubic structure. The presence of a liquid and a small grain size result in a pseudosuperplasticity of TZPs with an extension in tension of over 100% at 1200°C. High tensile ductility is obtained by grain size stability during high temperature deformation, which is achieved by suppressing the grain growth [15].
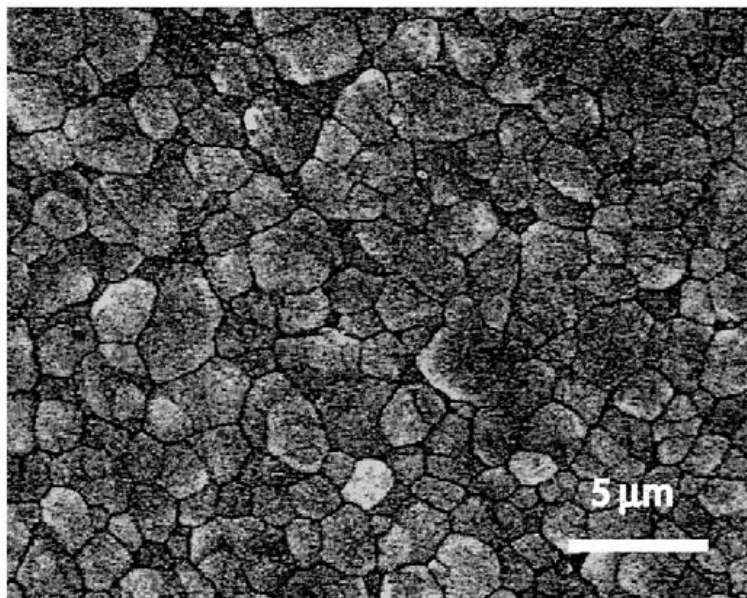
Figure 2.7 : Ytrria-stabilized tetragonal zirconia polycrystal (Y-TZP) [12].

2.5 Binary Phase Equilibria

An understanding of the phase equilibria of zirconia with other oxide system is fundamental to the application of zirconia as an engineering ceramic, both at low and high temperatures. Scientists have a great interest to the oxides which dissolve significant extent in zirconia. Also these oxides tend to stabilize the cubic fluorite phase due to their atomic radii [4].

MgO, CaO, Y_2O_3 and other rare earth oxides fall ion this category and have as a result been subjected to considerable scrutiny. However, even in such well studied systems there has been considerable disagreement as to the exact location of phase boundaries, probably arising as a consequence of differences in materials and experimental techniques. A further complication arises out of the very long time required to reach equilibrium at relatively high temperatures (1000-1400°C), a factor that has not always been appreciated [4].

2.5.1 ZrO$_2$-MgO phase diagram

Despite the generally accepted diagram for ZrO_2-MgO system is shown in Figure 2.8, but there is still a lot of discussion on the exact phase diagram for them. In this system there is little or no solubility MgO in m-ZrO_2. Between 1240°C and 1400°C, the solubility increases slightly around 1 mol% in a tetragonal solid solution field. However, beyond this temperature cubic solid solution field with a eutectic composition is present at 87 mol% ZrO_2 + 13 mol% MgO. With an appropriate cooling process, fully stabilized zirconia are retained to room temperature at the eutectoid composition [11].

Most commercial materials are produced with MgO content between 8 to 10 mol%, which results in a product with cubic and tetragonal phases. One of the most important advantage of retaining the tetragonal phase is material's strength and toughness increment because tetragonal phase can transform to monoclinic phase with the associated volume change. This type of materials is termed partially stabilized zirconia (PSZ) and by increasing amount of MgO, cubic phase being predominant, the material is considered fully stabilized zirconia (FSZ) [11].
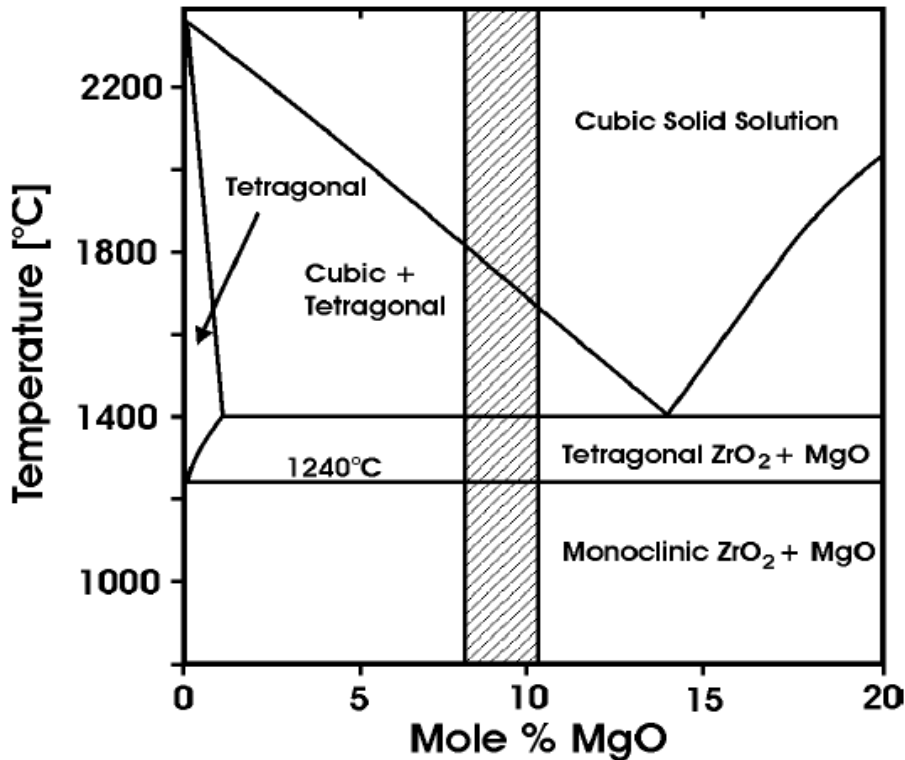
Figure 2.8 : Phase diagram of MgO-ZrO$_2$ [5].

Eutectoid decomposition of the cubic solid solution to the tetragonal solid solution and MgO is another feature that occurs upon cooling. During decomposition, MgO leaves ZrO$_2$ and migrates along grain boundaries and to intergranular voids. At still lower temperature, the tetragonal phase would decompose to monoclinic phase and therefore limiting their high temperature applications. Materials with low MgO content are very sensitive to large losses in strength and toughness when exposed to elevated temperature (around 1000°C) for long periods of time (>1000hr) [11, 22].

Complex decomposition and tertiary precipitation processes have also been reported to occur with aging of Mg-PSZ along with the development of quite some range of physical properties, for example, K$_{IC}$ ranging from 3 to 16 MPa.m$^{1/2}$ with lower values occurring in both un-aged and over-aged ceramic. In Mg-PSZ which has essentially c + t system, is developed a complex microstructure by aging. These changes include:

1) Tertiary t–phase precipitation

2) Some c→m transformation

3) Limited orthorhombic phase formation

14

4) Growth of an anion-ordered vacancy phase termed delta (δ) having the composition $Mg_2Zr_5O_{12}$.

This δ compound nucleates on the broad lenticular tetragonal-cubic phase boundary and grows with consumption of c-ZrO_2 and the t-δ-phase grain boundary is coherent. During growth of Mg-rich δ phase Mg amount is decreasing in t precipitates. It has been calculated roughly that the stress required for the $t \rightarrow m$ transformation decreases from 470 to 70 MPa with aging, in a linear fashion with δ-phase formation. Thus the improved mechanical properties of Mg-PSZ during aging can be defined by the precipitation of δ phase. Studies by a number of investigators have shown that the thermal expansion coefficient of MgO-PSZ could be reduced by heat-treatment, and so that the strength and fracture toughness could be increased [12, 23].

2.5.2 ZrO$_2$-Y$_2$O$_3$ phase diagram

This is the most common of the rare earth stabilized zirconia systems. Examining the low Y_2O_3 region of Y_2O_3-ZrO_2 phase diagram, shown in Figure 2.9. In this system the cubic phase field does not extend to lower temperature, but similar to that of MgO stabilized zirconia, undergoes an eutectoid decomposition [22].

There are two differences between this system and MgO-ZrO_2 system, first, the tetragonal solid solution is much larger, second, the $t \rightarrow m$ transformation temperature is significantly lower. Because of these two features, zirconia ceramic that are essentially 100% tetragonal phase can be produced with improved strength and fracture toughness. These materials have been termed tetragonal zirconia polycrystal (TZP) [11].

Other features of this system are that two types of t-ZrO_2 can be developed. At Y_2O_3 contents of approximately 4 mole-percent or less with increasing temperatures, a "transformable" t-phase field is encountered. This t-phase will transform to the m-phase on cooling. At Y_2O_3 contents above 4 mole-percent, a mixture of c-phase and an "untransformable" t-phase, labeled as t'-phase, can be displacively created. Because of the enhanced strength and toughness of ZrO_2 with Y_2O_3 contents between 2 and 4 mole-percent, the material has been examined for high-temperature structural. Further additions of Y_2O_3 create a homogeneous c-phase that is stable from room temperature to the melting point [11].

15
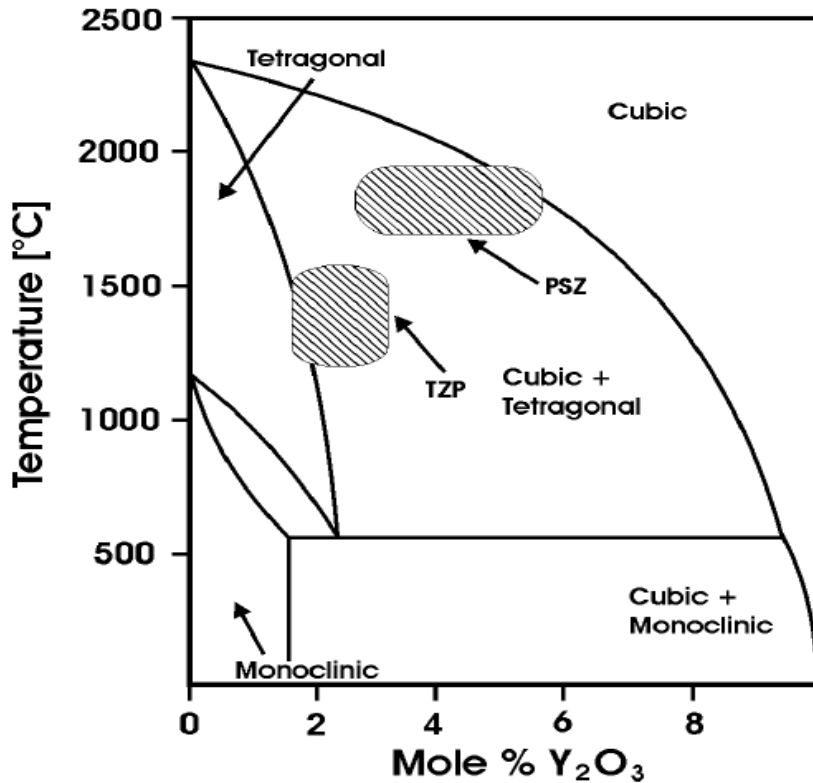
Figure 2.9 : Phase diagram of ZrO_2-Y_2O_3 [5].

At higher Y_2O_3 doping, the material exhibits an ordered $Zr_3Y_4O_{12}$ phase at 40 mol% Y_2O_3, a eutectoid at a temperature $< 400°C$ at a composition between 20 and 30 mol% Y_2O_3, a eutectic at 83 ± 1 mol% Y_2O_3, and a peritectic at 76 ± 1 mol% Y_2O_3 [1].

2.5.3 ZrO_2-CaO phase diagram

This system is similar to the MgO-ZrO_2 system, but unlike it, there is a general agreement on the formation of several stable intermediate compound. At lower temperature there are two phases : $CaZr_4O_9$ and $CaZrO_3$, however the last one stable to its melting point [22].

Below 2400°C the tetragonal solid solution is stable up to a CaO content of about 6 mole%, but on cooling the system passes through region B, in which the tetragonal and monoclinic solid solutions are simultaneously stable; continued cooling results in a monoclinic solid solution + $CaZr_4O_9$. Above the 1140°C (the eutectic transformation temperature) at between 6 and 17 mol% of CaO, there are two phase field tetragonal ss + cubic ss, which indicate the phase stability of CaO-PSZ.
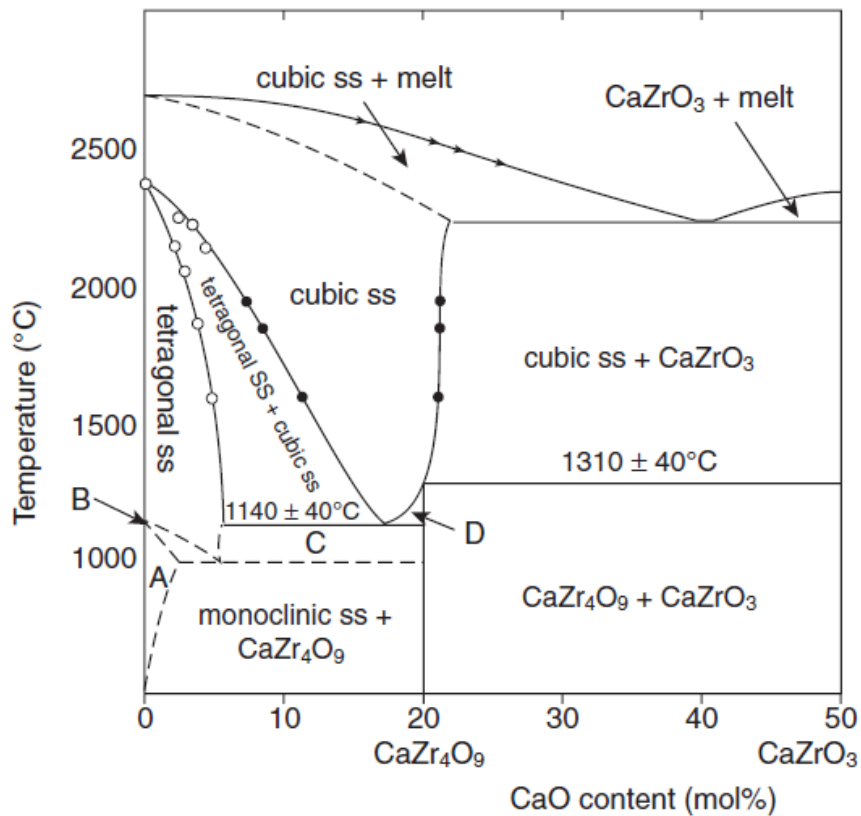
Figure 2.10 : ZrO_2-CaO phase diagram [10].

Tetragonal solid solution is changed to monoclinic solid solution by quenching below 1140°C, which matrix is still cubic. In contrast, slow cooling to 1000°C results in the phase assembly t_{ss} + $CaZr_4O_9$. Within the cubic phase field (17 − 20mol% CaO) a similar reaction takes place, showing transformation from c ss to t ss between 1140 and 1000°C, and from t_{ss} to m_{ss} below 1000°C [10, 22].

2.6 Transformation Toughning of Zirconia

Garvie, Hannink and Pascoe in publishing their seminal article 'Ceramic steel' were the first to realize that by using the tetragonal → monoclinic phase transformation of metastable tetragonal particles, zirconia based ceramics enhance their both strength and toughness. The tetragonal → monoclinic transformation is induced by the stress field ahead of crack. The volume change and developing of shear strain in the martensitic reaction were recognized as opposing the opening of the crack and therefore acting to increase the resistance of the ceramic to crack propagation [4].

There are three different mechanisms for increasing toughness and strength:

1. Microcracking

2. Stress induced transformation toughening

3. Compressive surface layer

2.6.1 Microcracking

The reverse t→m transformation, which occur with volume increasing (3-5%) during cooling the zirconia, results in significant strain, which can be only accommodated by the formation of cracks [15].
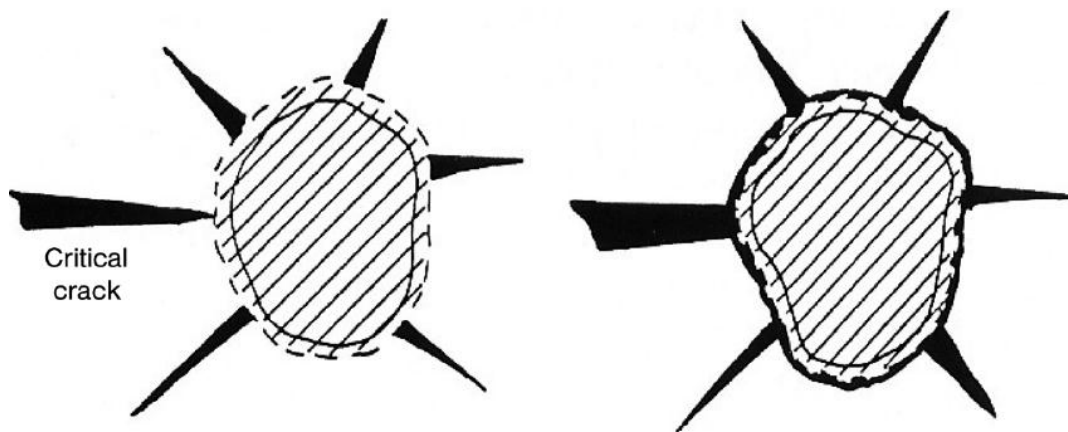
Figure 2.11 : Microcrck formation around a transformed zirconia particle [15].

Tangential stresses are generated around the transformed particle which induce microcracks in the matrix; these by their ability to extend in the stress field of a propagation crack or to deflect the propagation crack can absorb or dissipate the energy of crack, thereby increasing the toughness of the zirconia. For obtaining optimum condition, particles should be large enough to transform, however, be only small enough to cause limited microcrack development [4].

2.6.2 Stress induced transformation toughening

During cooling zirconia form above 1200°C to room temperature the t→m transformation should occur. However, if the grians fine enough or a constraiting pressure is exerted on it by the matrix, the zirconia particle can be retained in the metastable tetragonal form [4].

The metastable tetragonal particle can be transformed by the stress field at the tip of a propagating crack. The volume change and shear strain associated with the transformation oppose the opening of the crack, thus increasing the resistance of the

ceramic to crack propagation (Figure 2.12) [15]. Therefore, it can be said phase transformation toughening originates in the presence of large tensile stresses around a crack, which can destabilize the tetragonal phase in the vicinity of the crack, forming a transformation zone [24].
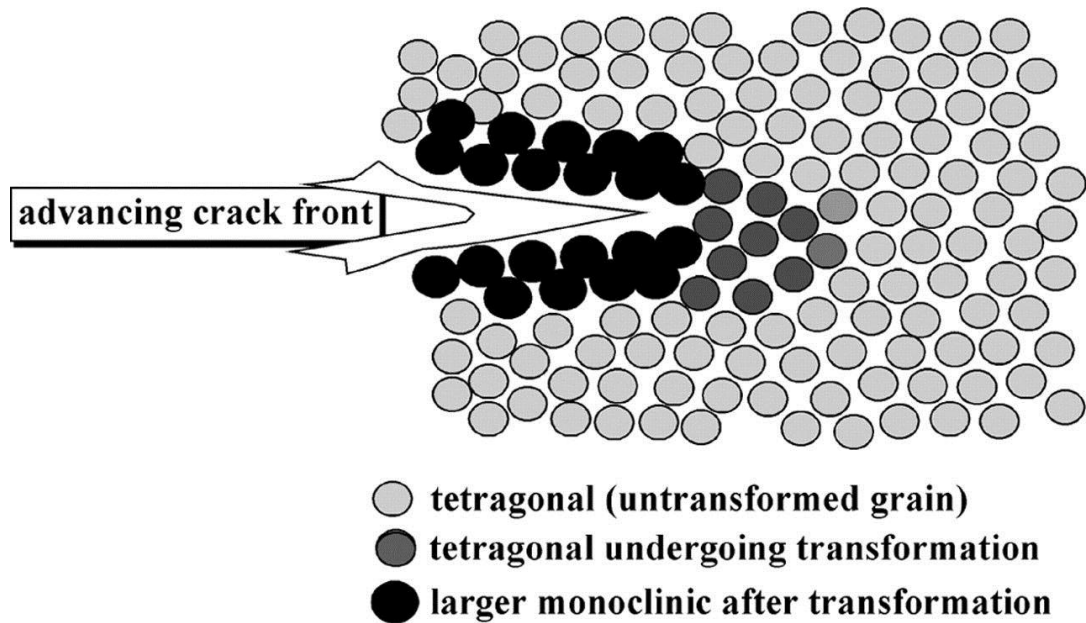
Figure 2.12 : Schematic illustration of stress-induced transformation toughening [25].

If a crack were to be extended under the stress, then large tensile stresses would be generated around the crack, especially ahead of the crack tip. These stresses would release the matrix constraints such that the transformable tetragonal inclusions would transform to monoclinic, and the resultant volume expansion (3%) and shear strain (1–7%) would lead to the generation of a compressive strain in the matrix. If this were to occur in the vicinity of the crack, then extra work would be required to move the crack farther. There exists a size interval for zirconia particles, where the tetragonal particles can be transformed by stress. If the particles are less than critical size they will not transform, but if they are larger than the critical size then they will transform spontaneously [15].

2.6.3 Compressive surface layers

An interesting characteristic of transformation toughened zirconia ceramics is the formation of compressive layers on their surface. Surface tetragonal grains are not constrained by the matrix, and can transform to monoclinic spontaneously or due to

abrasive processes that can induce compressive stresses at a depth of several microns under the surface.

The surface phase transition and the consequent surface hardening may have a relevant role in improving the mechanical and wear properties of zirconia parts, the thickness of the transformed layer being one of the limit conditions. Progresses in t→m surface transformation may originate surface cracking, followed by ejection of grains from the surface with catastrophic effects on mechanical behaviour and joint wear [25].
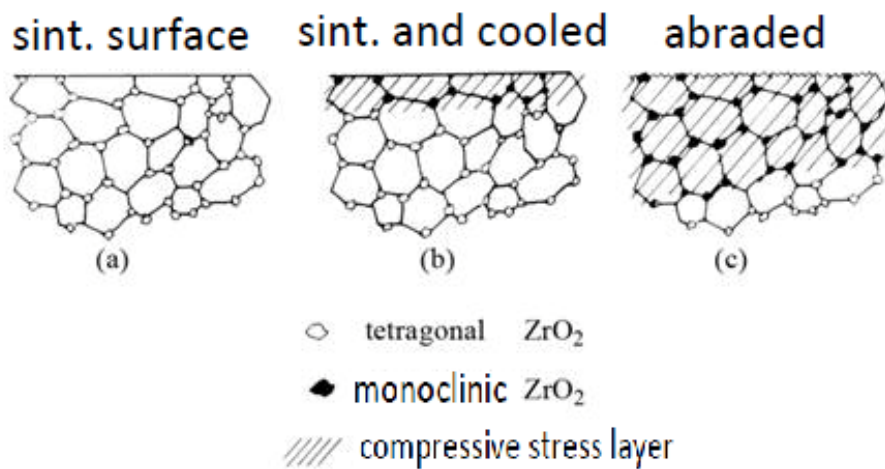
Figure 2.13 : Diagram of a section through a free surface at (a) the sintering temperature. on cooling, particles of ZrO_2 near the surface (b) transformation due to reduced constrain, developing a compressive stress in the matrix. The thickness of this compressively stressed layer can be increased (c) by abrasion or machining [4].

3. ZIRCONIA BASED REFRACTORY MATERIALS

3.1 Introduction

Zirconia (ZrO_2) is usually obtained trough a chemical process involving zircon or by fuding zircon with coke in an electrical furnace. Zirconia has performed as an ideal refractory materials for many years. It has an extremely high melting point (2680°C) an excellent chemical inertness. However the tetragonal-monoclinic phase transformation, which associated with volume change, and its high cost preclude the use of zirconia. The phase change transition results in spontaneous failure of the zirconia crystal by cracking and disintegration of the refractory shape [4, 26].

The fundamental cracking problem can be overcome by milling monoclinic zirconia to affine size (less than one micron) and disperse it within a refractory body so that destructive micro-cracking is avoided. The other approach is to stabilized the cubic structure with lime, magnesia and yttria. The cubic form of zirconia has a uniform thermal expantion, whereas themal expansion of the other polymorphs reflect volume changes which occur upon heating. A disadvantage of stabilized zirconia is its tendency to thermally age. The stabilizer can be migrate out of the structure when the material is heated to high temperature between 800-1400°C for long period of times [26].

Zircon is mineral which has about 67% zirconia and 23%s silica. Zircon refractories are made by blending beneficiated zircon sand, milled zircon sands and a plasticizer, forming and firing to 1500-1650°C. Brick consisting essentially of zircon are typically made by forming process called impact pressing [26].

3.2 Refractory Castables

In the family of monolithic refractories, refractory castables comprise a large group of materials that have evolved and grown significantly in the past 30 years. Progressing from rather simple mixes, refractory castables today comprise some very complex and technical formulations, finding use in a variety of very demanding and

severe industrial applications. In this time period, refractory castables have gained in market share and, in many instances, have supplanted brick and shaped refractories and become, in many applications, the refractories of choice because of enhanced performance and ease of installation.

Refractory castables are premixed combinations of refractory grain, matrix components, bonding agents, and admixtures. The vast majority of castables are supplied as bagged, blended mixes though some very simple formulations are still field blended for use in low-temperature and noncritical applications. At the point of installation, the castable is mixed with a liquid (typically water) and vibrated, poured, pumped, or pneumatically shot into place to form a refractory shape or structure that becomes rigid because of hydraulic or chemical setting. A shematic of castble refractories process is shown in Figure 3.1 [27].

There are some zirconia castable refractories mentioned here:

NARCON ZRAL: A 60% zirconia castable with excellent corundum resistance. Zoning aluminum furnace belly bands with NARCON ZARL has proven to be very successful in furnaces prone to corundum formation.

THOR AZSP ADTECH: A pumpable, low moisture fused zirconia-mullite castable with silicon carbide addition. The zircon is tied up with the mullite and will not reduce. It has exceptional resistance to alkalis, chlorides and sulfates. It has excellent abrasion high refractories [26].

3.3 Zirconia Refractory Applications

Because of high cost of zirconia refractory, they are only used in critical applications, such as metering nozzoles used in continuous casting and inerts in the bore area of slide gates. Some zirconia is used to make crucibles for refining special alloys where purity of the molten metals is of concern. The main use of zirconia in the refractories industry, in terms of additive to increase the thermal shock or slag resistance of the materials [26].

3.3.1 Zirconia brick

Zirconia bricks are used primarily for custom high-temperature furnace linings, supports and heat shields. Zirconia bricks withstand operating temperatures greater

than 2000°C (3630°F) with capacity to spare. Quartz melting and synthetic crystal growing are typical applications [26].
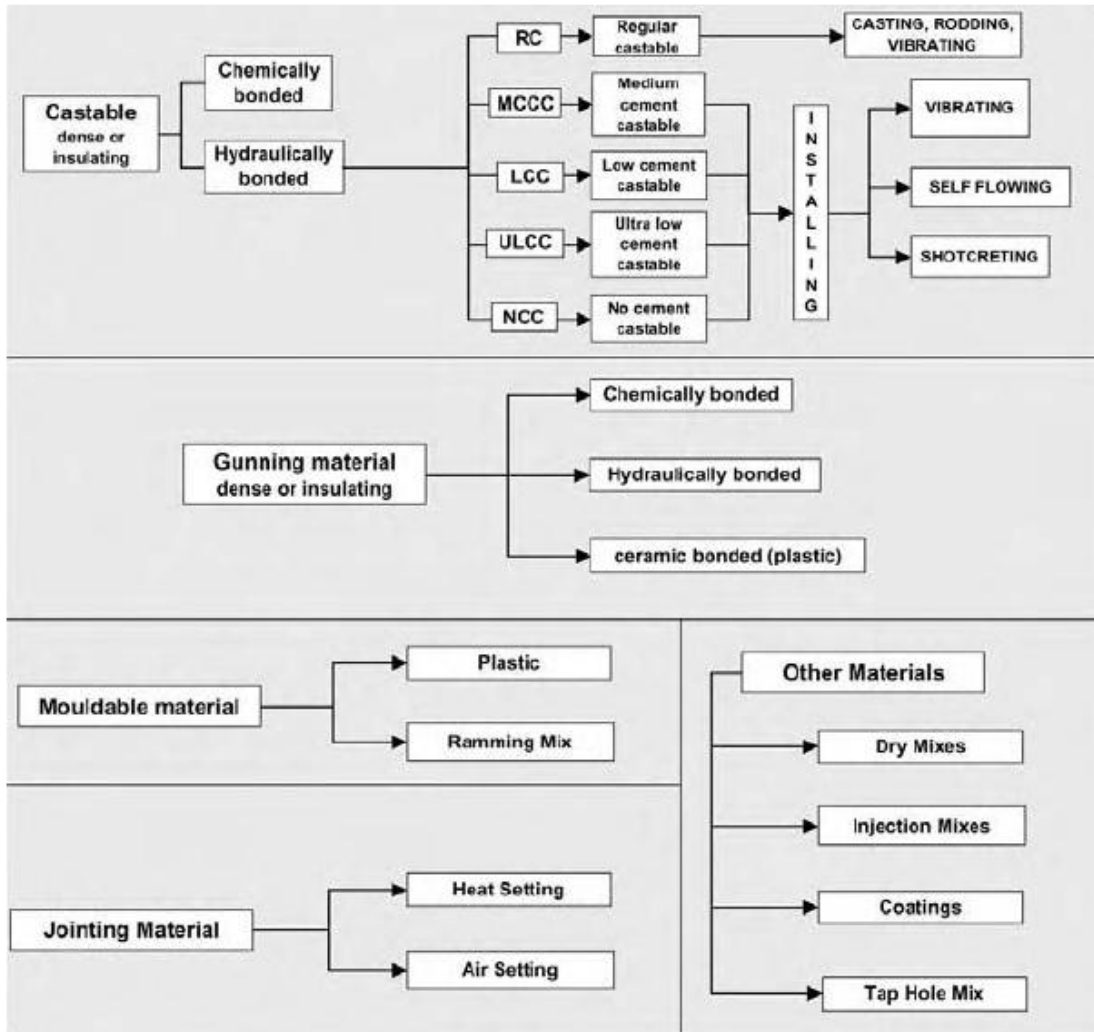
Figure 3.1 : Subdivision of unshaped refractory products schematically [27].

Figure 3.2 : Standard zirconia bricks [30].

3.3.2 Zirconia nozzle

Zirconia is usually utilised in nozzle in the slag contact zone because of its high resistance to corrosion. The improvements made in the continuous casting of steel and the long casting time has resulted in the demand of use of zirconia based nozzles. The casting technique ensures that the insert is tightly fitted in the nozzles and this process helps to reduce crack formation and prevents cracks from opening up should they happen to take place [28]. Zirconia based nozzles have some advantages such as [29]:

1) High erosion and corrosion resistance

2) High termal shock resistance

3) High density

4) Exact flow area dimensions
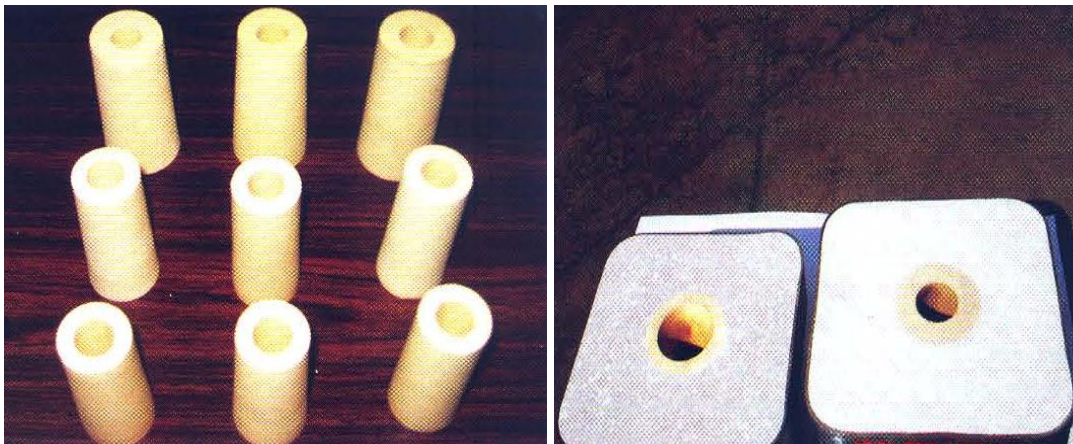
Figure 3.3 : Zirconia based nozzles [29].

3.3.3 Zirconia tube

Zirconia coarse grain tubes are used primarily in induction heating applications. They are ethier pressed or cast, and composed of calcia, yttria or magnesia stabilized zirconia. By varying the composition, manufacturing method, grain size, mass and shape, they are manufactured to the unique requirements of applications [30].

3.3.4 Zirconia burner block

Oxy-fuel firing for glass is becoming more common because it reduces NOx emissions, reduces capital expenditures and imorove glass quality. When feul oil is used, the life of typical burner blocks are less than six month. This is due to the high

temperature generated by the burner and the contaminants present in the oil. Zirconia burner blocks provide the added resistance to corrosion and withstand high temperatures found in this environment. Using zirconia, burner block life is extended to more than one year [30].

Figure 3.4 : Zirconia tube [30].

4. EXPERIMENTAL PROCEDURE

4.1 Raw Materials

4.1.1 Zirconia (ZrO₂)

In this study two types of zirconia powders were used, monoclinic and tetragonal stabilized zirconia, which particle size and phase analysis of them mentioned below.

4.1.1.1 MgO stabilized zirconia

Most of the materials used in the present work were Supplied by Metamin A.S. industry. MgO stabilized zirconia with different particle sizes are shown in Table 4.1. particle size distribution was determined by Malvern Mastersizer 2000 Laser Particle Sizer.

Table 4.1 : Particle size distribution of MgO stabilized zirconia.

Powder	d(0.1) (μm)	d(0.5) (μm)	d(0.9) (μm)
7-9 micron	3.7	12	27
-100 mesh	76	131	220

Table 4.2 : Chemical analysis of MgO stabilized zirconia.

Properties			
Chemical Analysis (wt%)	XEPOS EDSXRF	ZrO_2 MgO	94.73 4.10
Density (g/cm³)	Pycnometer		5.54
Phase Analysis (%)	Bruker XRD		65.5 tetragonal+cubic, 34.5 monoclinic

4.1.1.2 Monoclinic Zirconia

Baddeleyite has monoclinic crystal structure between room temperature and 1170°C. Baddeleyite powders was supplied by Metamin A.S. industry. X-ray diffraction pattern (XRD) of baddeleyite powder is shown in Figure 4.2. According to phase

analysis, high purity powders were used for the processing (most of the peaks are monoclinic). Figure 4.1 shows the particle size distribution of zirconia monoclinic powder, which it indicates : d(0.1)=3.87 µm, d(0.5)=6.57 µm, d(0.9)=11.04 µm.
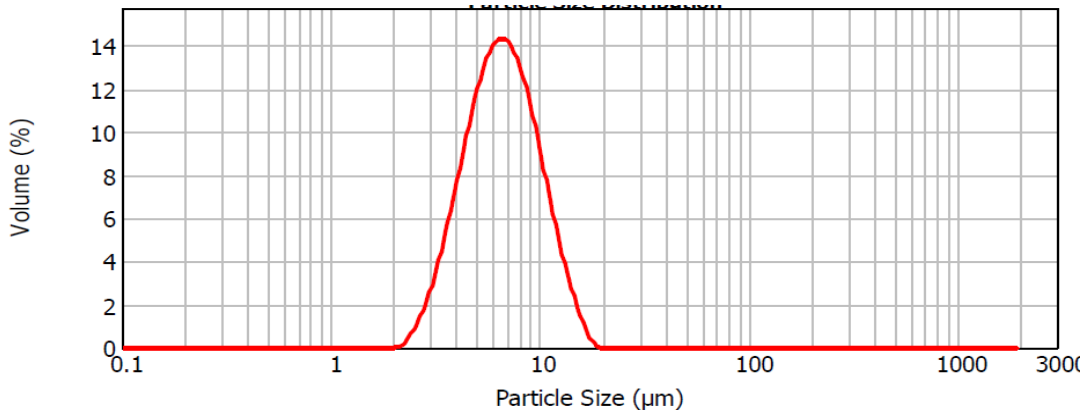
Figure 4.1 : Particle size distribution of ZrO_2 powder.
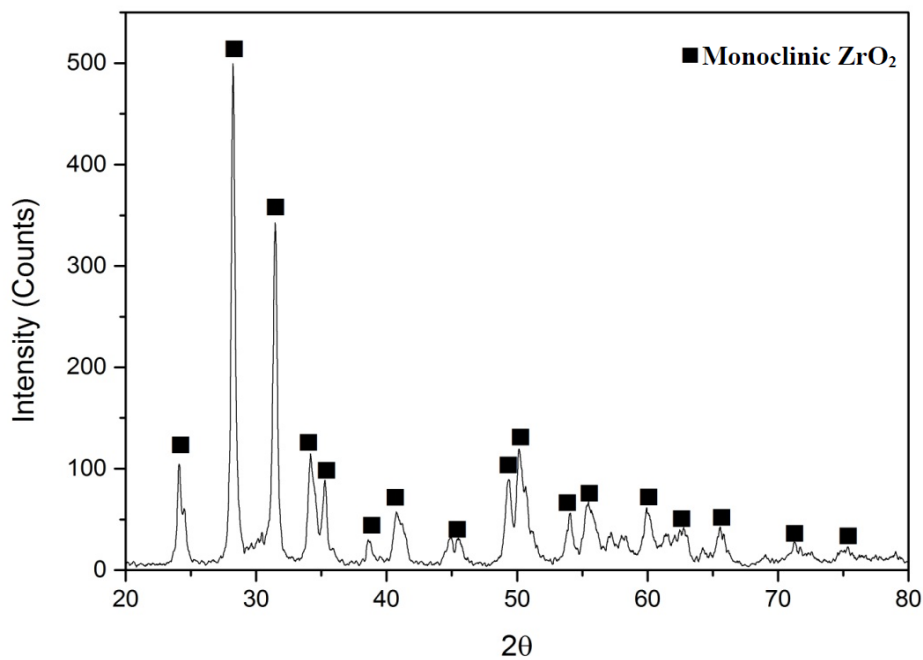
Figure 4.2 : X-ray diffraction pattern (XRD) of baddeleyite powder.

4.1.2 Dead burned magnesium oxide (Sintered MgO)

Magnesium oxide (MgO) or magnesia is a white powder with high melting point temperature (2800°C). Because of this property, it is used as zirconia stabilizer in high temperature refractories. Dead burned magnesium oxide purchased from Kumas Manyezit A.S., which has $CaMgSiO_4$ as impurity. Chemical analysis and X-ray diffraction pattern (XRD) of MgO powder are shown in Table 4.3 and Figure 4.4,

28

respectively. Figure 4.3 shows the particle size distribution of MgO powder, which it indicates : d(0.1)=4.84 µm, d(0.5)=29.66 µm, d(0.9)=66.53 µm.
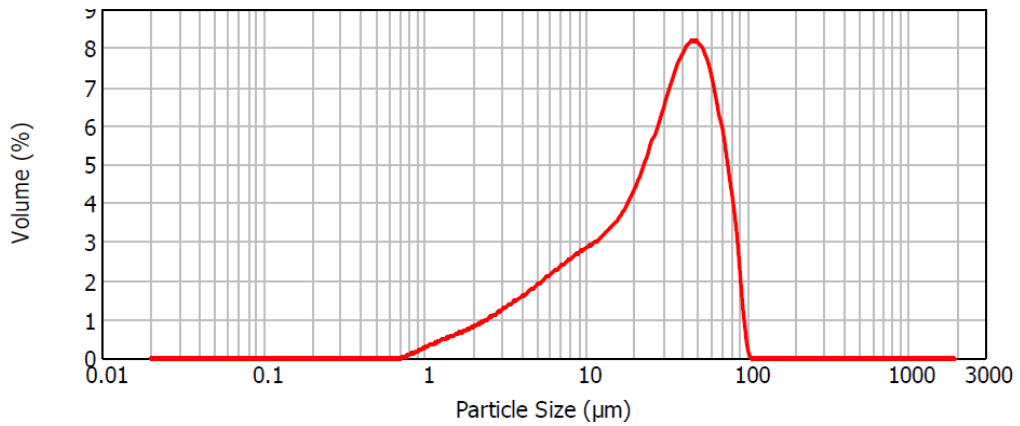
Figure 4.3 : particle size distribution of dead burned MgO powder.
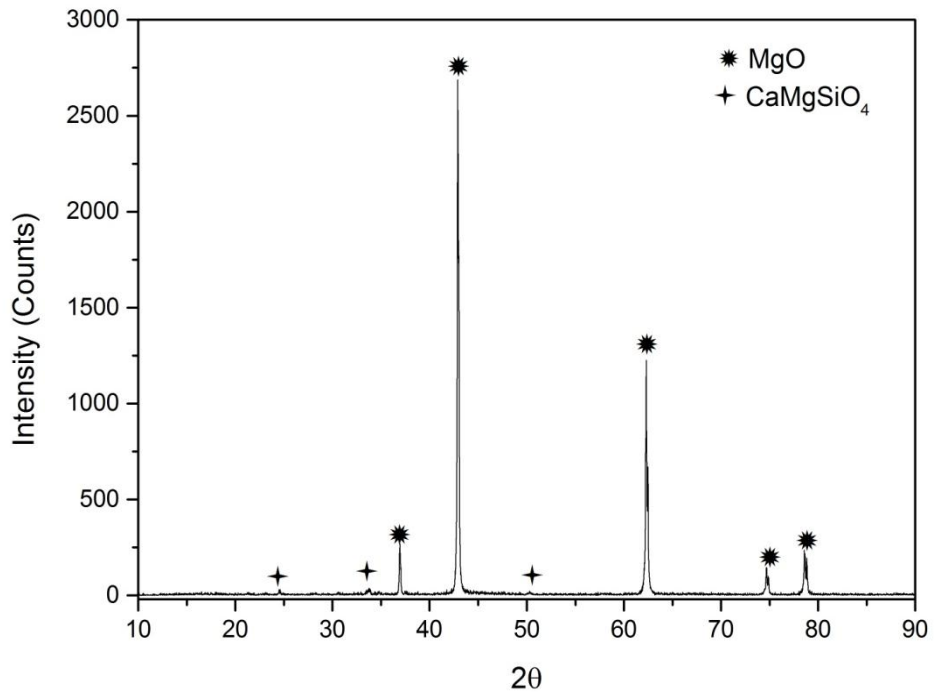
Figure 4.4 : X-ray diffraction pattern (XRD) of dead burned MgO.

Table 4.3 : Chemical analysis of dead burned MgO.

Oxide	Weight percent
MgO	96.53
SiO_2	1.30
CaO	1.69
Fe_2O_3	0.36
C/S	1.3

4.1.3 Titanium dioxide (TiO₂)

Titanium dioxide (TiO_2), also known as titania, is a white powder with three crystal structure (rutile, anatase, brookite). It is supplied by Metamin A.S. industry. Figure 4.5 shows the particle size distribution of TiO_2 powder, which it indicates : d(0.1)=0.52 µm, d(0.5)=1.24 µm, d(0.9)=2.91 µm. Figure 4.6 shows the X-ray diffraction (XRD) pattern of TiO_2. It can be seen from it that TiO_2 powder include only rutile phase.
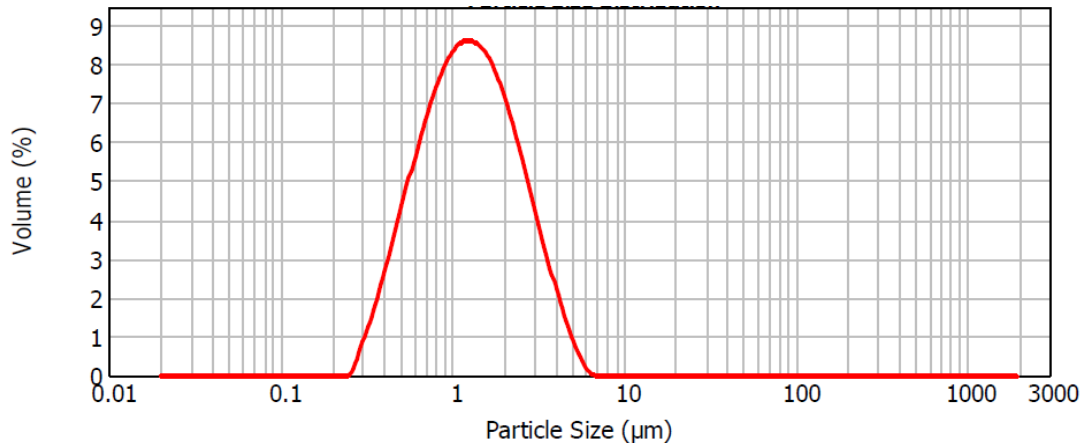
Figure 4.5 : Particle size distribution of TiO_2 powder.
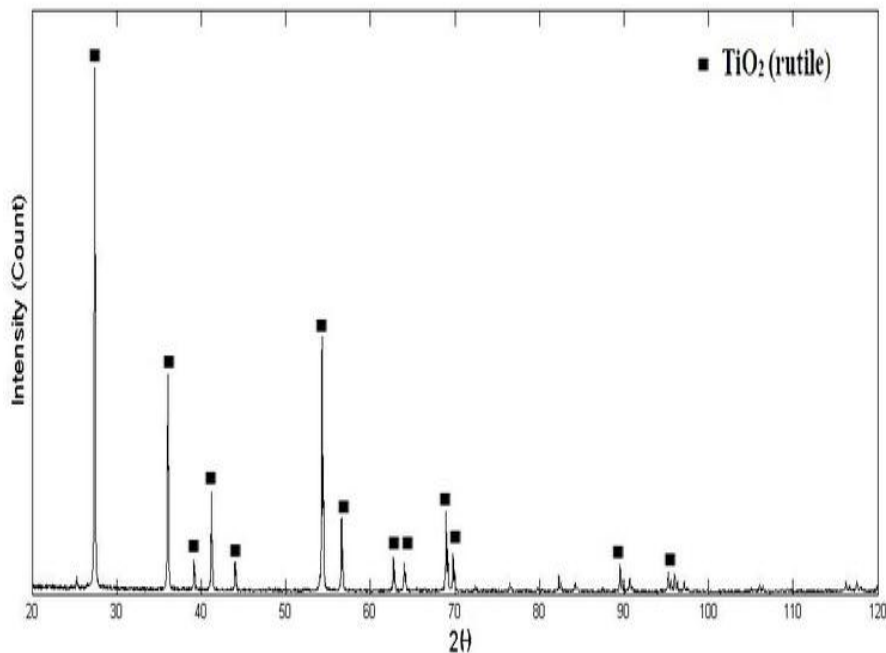
Figure 4.6 : X-ray diffraction pattern (XRD) of TiO_2.

4.1.4 Silicon Nitride (Si₃N₄)

Silicon nitride (Si_3N_4) is a high melting point powder (1900°C) and chemically inert. It is purchased from Metamin A.S. industry. Figure 4.5 shows the particle size distribution of Si_3N_4 and the results are : d(0.1)=4.07 μm, d(0.5)=24.34 μm, d(0.9)=57.81 μm. the X-ray diffraction pattern of powder is shown in Figure 4.7. As seen in Figure 4.8, the peaks of free silicon are observed as impurity, however, silicon nitride peaks are performed majority.
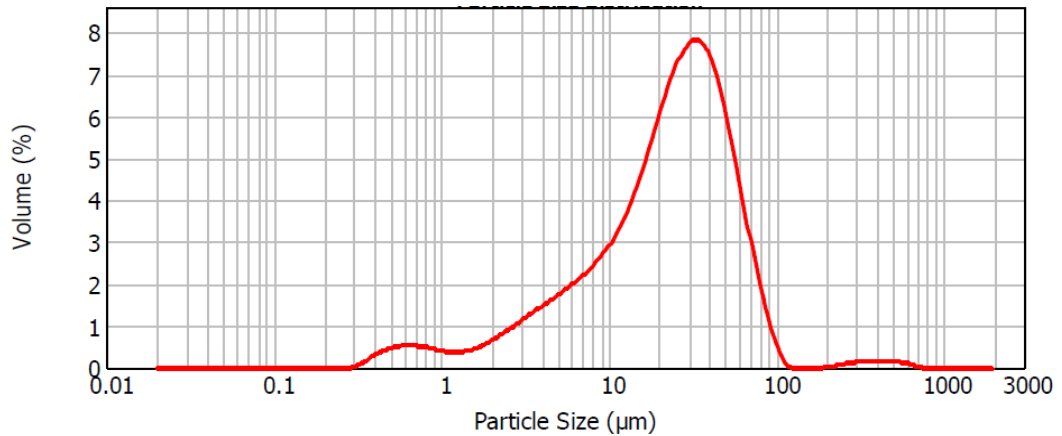
Figure 4.7 : Particle size distribution of Si_3N_4 powder.
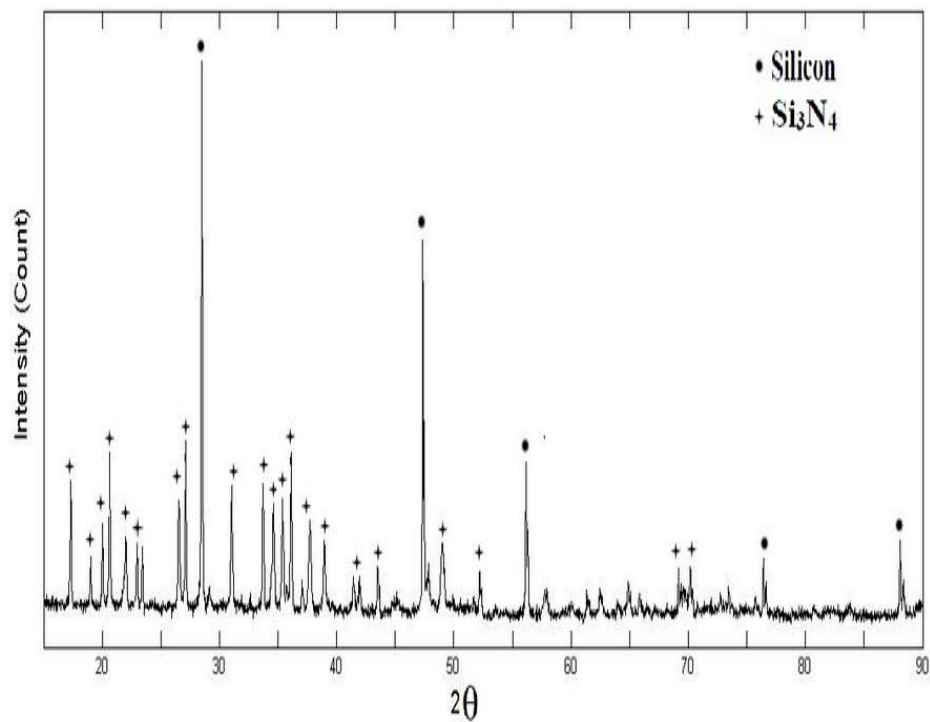
Figure 4.8 : X-ray diffraction (XRD) pattern of Si_3N_4.

4.1.5 Silicon carbide (SiC)

Silicon carbide (SiC), also known as carborundum, is a high melting point powder (2730°C) with grey color. Figure 4.9 shows SiC powder's particle size distribution. According to analysis the particle size distribution of SiC is : d(0.1)=0.74 μm, d(0.5)=2.44 μm, d(0.9)=5.85 μm. it purchased from Metamin A.S. industry.
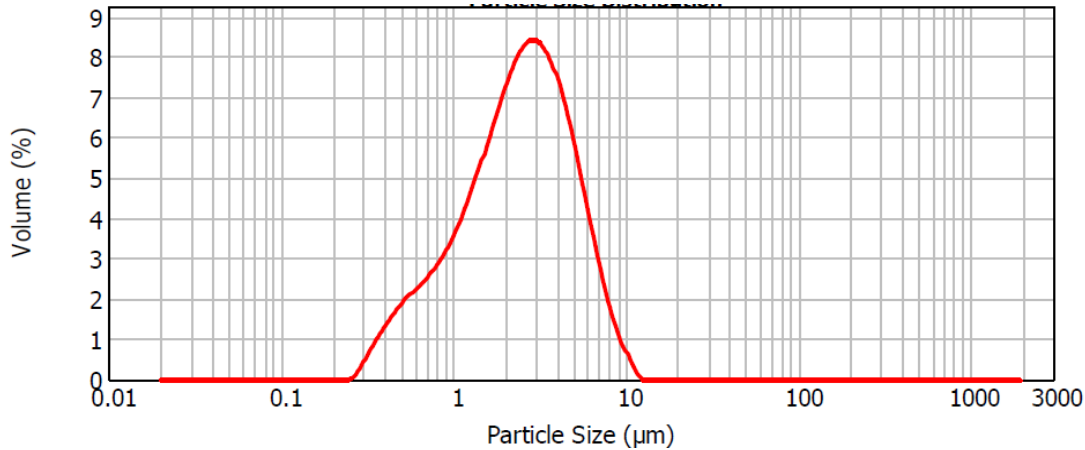
Figure 4.9 : Particle size distribution of SiC powder.

4.1.6 Other additives

4.1.6.1 PVA (Polyvinyl alcohol)

Polyvinyl alcohol or PVA is a water-soluble and white (colorless) polymer. It has the idealized formula $[CH_2CH(OH)]_n$. PVA is common additive for pressing process in ceramic materials. Table 4.4 shows polyvinyl alcohol properties, which Supplied by Metamin A.S. industry in liquid state.

Table 4.4 : Properties of polyvinyl alcohol.

Property		Value
Density	g/cm^3	1.08
pH		6
Viscosity	mPa.s	1500

4.1.6.2 Dispersant (Polyacrylate)

Dispersant was added to suspension, which prepared for wet milling, to improve the separation of particles and to prevent settling and clumping. Density and viscosity of dispersant are 1.16 g/cm^3 and 14000 mPa.s, respectively.

4.2 Sample Preparation

Figure 4.10 below shows a schematic of the preparation process:

```
┌──────────────┐  ┌──────────────────┐  ┌──────────────┐  ┌──────────────────┐
│     MgO      │  │    Additive      │  │    ZrO₂      │  │  Other additives │
│              │  │ (TiO₂, Si₃N₄,SiC)│  │              │  │ (PVA, Dispersant)│
└──────────────┘  └──────────────────┘  └──────────────┘  └──────────────────┘
```

MgO — Additive (TiO_2, Si_3N_4, SiC) — ZrO_2 — Other additives (PVA, Dispersant)

Ethanol → Wet ball mill and mixing → 4 hr

Drying (120°C, 12 hr)

Compaction (22 MPa)

Binder burnout

Sintering & Aging

Characterization

Density   XRD   Hardness   3.pont bending   Fracture toughness   SEM

Figure 4.10 : Schematic of the preparation process for the samples.

4.2.1 Composition of specimens

4.2.1.1 Monoclinic zirconia (with MgO as stabilizer) with addition of Si_3N_4

Starting powders were monoclinic zirconia containing 3.12 wt% MgO (equal to 8 mol%) as stabilizer and Si_3N_4. Zirconia and MgO were mixed with 0, 5, 10 or 15 wt% Si_3N_4 powders, 3 wt% PVA and 0.7 wt % dispersant and ball-milled in ethanol for 4 hours. The green compacts of the mixed powders were sintered at 1600°C. With increasing the content of Si_3N_4 the amount of monoclinic zirconia was decreased.

4.2.1.2 Monoclinic zirconia (with MgO as stabilizer) with addition of TiO_2

The powders used in these samples were monoclinic zirconia, 3.12 wt% MgO as stabilizer and 0, 5, 10 or 15 wt% TiO_2 powder. Powders were blended with 3 wt% PVA and 0.7 wt % dispersan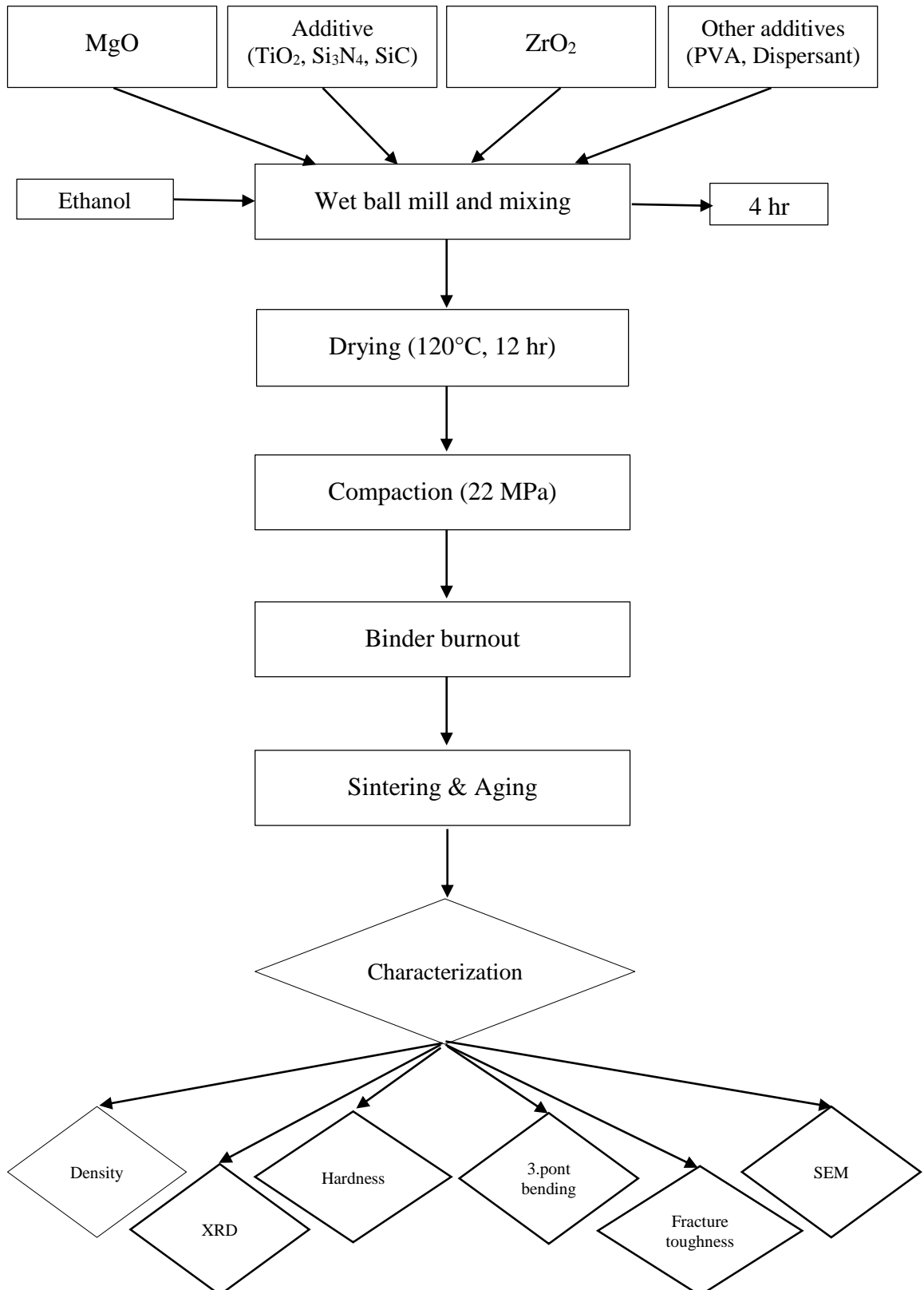t by ball-milling in ethanol. After drying specimens were pressed and sintered at 1400°C and 1600°C. With increasing the content of TiO_2 the amount of monoclinic zirconia was decreased.

4.2.1.3 Stabilized zirconia powder (tetragonal+cubic) with addition of TiO_2

Stabilized zirconia powder and 0, 5, 10 or 15 wt% TiO_2 were used for preparing specimens. Powders were mixed with 3 wt% PVA and 0.7 wt % dispersant, and ball-milled in ethanol. The green compacts of the mixed powders were sintered at 1400°C and 1600°C. With increasing the content of TiO_2 the content of monoclinic zirconia was decreased.

4.2.1.4 Monoclinic zirconia (with MgO as stabilizer) with addition of SiC

Starting materials were monoclinic zirconia, 3.12 wt% MgO (equal to 8 mol%) as stabilizer and 0, 5, 10 or 15 wt% SiC powder. Powders were blended with 3 wt% PVA and 0.7 wt % dispersant by ball-milling in ethanol. After drying, the blended powders were pressed under 22 MPa and sintered at 1600°C. The dopant amount was based on the content of zirconia in the specimens.

4.2.2 Wet ball milling

In order to obtain powder which will compact and sinter uniformly to a high density, it is necessary to mill the powder. For this study a planetary ball mill was used which

shown in Figure 4.11 (a). Figure 4.9 (b) and (c) shows YSZ milling balls (in 6.35mm diameter) and zircon bowl (FRITSCH^{TM}) respectively. 100g of powder was suspended in ethanol with 700g of YSZ milling balls, 3g PVA and 0.7g dispersant were added. All specimens were ball milled 4 hours. After milling the powder was dried at 120°C for 4 hours using drier. Figure 4.12 shows the motion of the balls and the powder. Since the rotation direction of the bowl and the turn disc are opposite, the centrifugal forces are alternately synchronized.
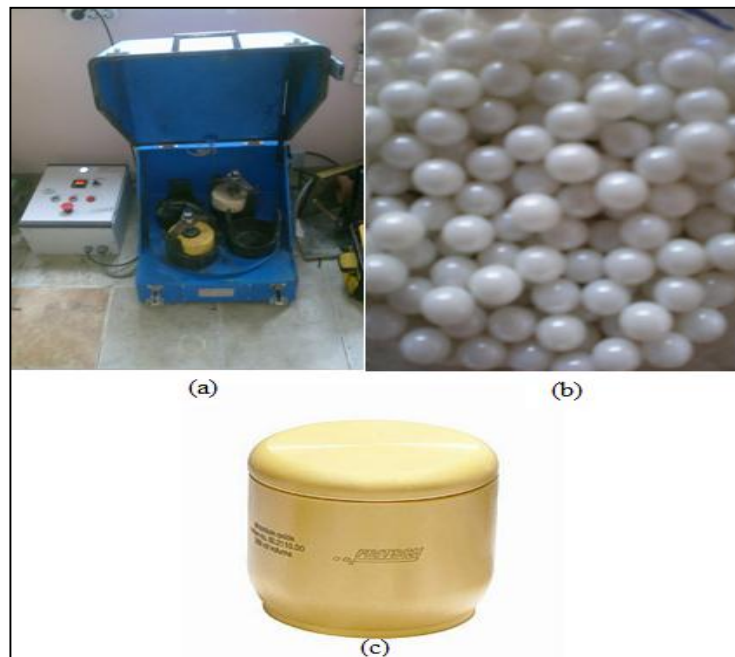

Figure 4.11 : (a) Plantery ball mill (b) YSZ milling balls (c) Zircon bowl (FRITSCH^{TM}).
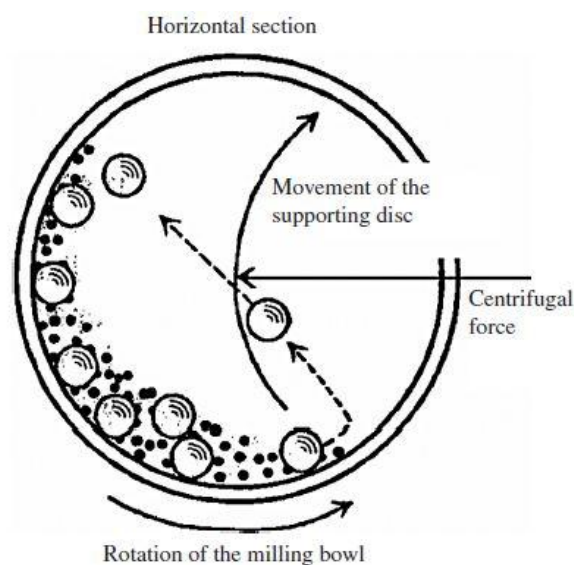
Figure 4.12 : Schematic view of motion of the ball and powder mixture [21].

4.2.3 Compaction

After milling, it is necessary to form the powder into shapes suitable for sintering and subsequent mechanical test. Approximately 15g of mixed powders were uiaxially die-pressed under a pressure of 220 bar (=22MPa) at room temperature. Zinc Stearat was applied to the walls of the die to take the samples out of the die easily. The sesulting samples dimentions were about 51*9*15mm. Figure 4.13 shows the uniaxial hydraulic press.

Figure 4.13 : APEX^{TM} 3010/4 one-action hydraulic press.

4.2.4 Binder burnout

After pressing, the green bodies were all heated up to 600°C to remove the 3 wt% of PVA. This was done in a furnace in air at a heating and cooling rate of 2°C/min. Figure 4.14 shows Protherm^{TM} furnace which used for removing binder. The samples were kept at 600°C for an hour.

4.2.5 Sintering and aging

4.2.5.1 Si$_3$N$_4$ added specimens

Sintering of Si$_3$N$_4$ added samples were performed in a furnace in nitrogen atmosphere at 1600°C for 2 hours. Green bodies were heated to the sintering temperature at a rate of 5°C/min where specimens were held for two hours before cooling down to room temperature at a rate of 5°C/min. Figure 4.15 shows Linn^{TM} HT-1800 high temperature controlled atomsphere furnace.

Figure 4.14 : Protherm^{TM} binding removing furnace.

Figure 4.15 : Linn^{TM} HT-1800 high temperature controlled atomsphere furnace.

4.2.5.2 TiO₂ added specimens

Sintering of TiO₂ added specimens were carried out in two different process:

a) The green compacts were heated up to 1400°C at a rate of 5°C/min, and sintering was performed with hold time of 2 hours at 1400°C in air. Then, samples cooled down to room temperature at a rate of 5°C/min. Samples were sintered in Prothem^{TM} sintering furnace shown in Figure 4.16.

Figure 4.16 : Protherm^{TM} sintering furnace.

b) After removing the binder, the green bodies were heated to 1300°C at a rate of 5°C/min. Heating rate was directly changed to 2°C/min, which continued to 1600°C. sintering was carried out at 1600°C with hold time of 5 hours in air. Aging was performed at 1100°C for 4 hours before samples cooling down to room temperature at a rate of 5°C/min. Figure 4.17 shows this sintering process as a graph.

4.2.5.3 SiC added samples

Sintering of SiC added specimens were carried out in a furnace in argon atmosphere at 1600°C. Green bodies were heated to the sintering temperature at a rate of 5°C/min where samples were held for two hours before cooling down to room temperature at a rate of 5°C/min.
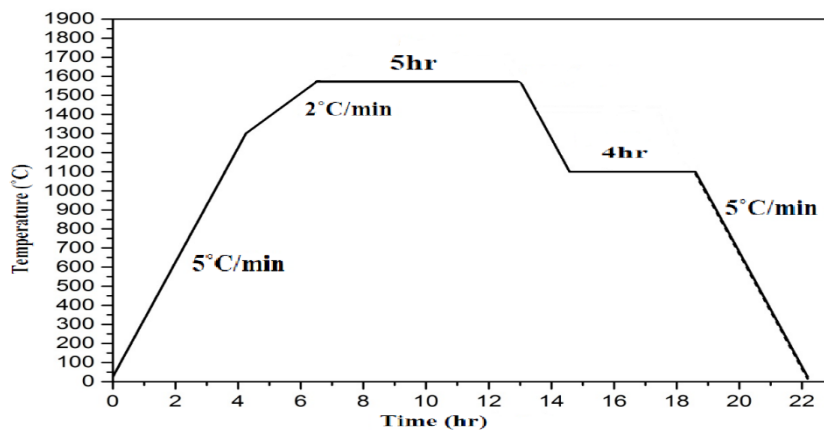

Figure 4.17 : Sintering process of portion of TiO$_2$ added samples.

Zirconia

Monoclinic ZrO_2

Tetragonal stabilized ZrO_2

Si_3N_4

SiC

TiO_2

TiO_2

1600˚C

1600˚C

1400˚C

1600˚C & Aging

1400˚C

1600˚C & Aging
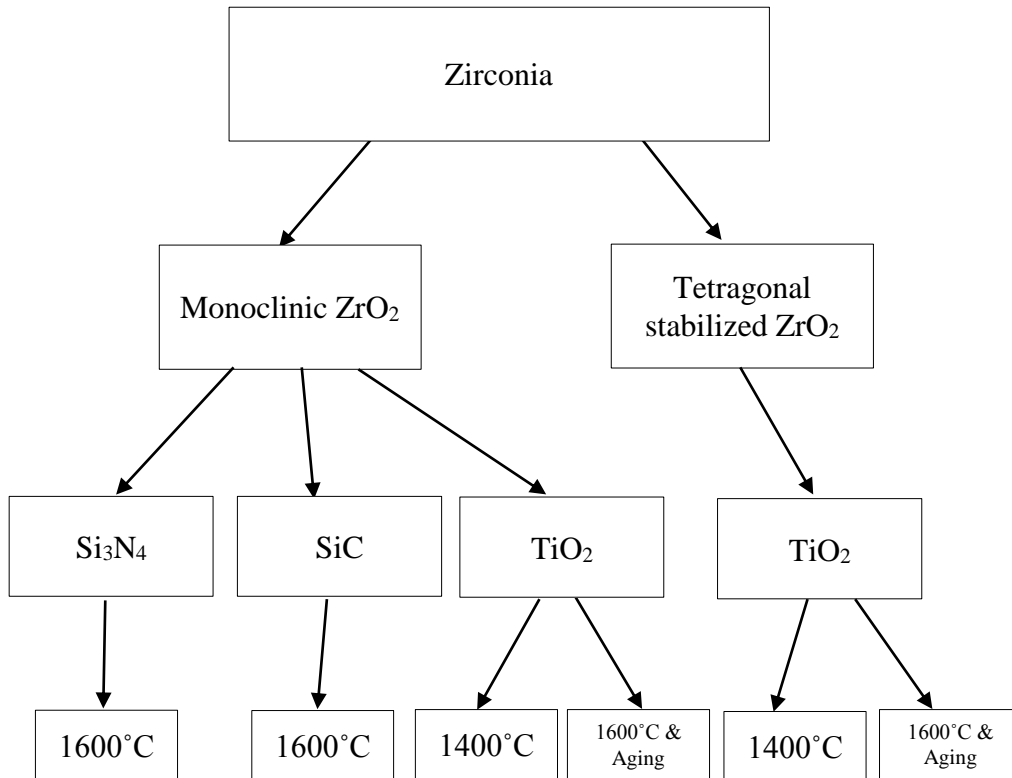
Figure 4.18 : Sample types and sintering temperature.

4.3 Characterization

4.3.1 Metallographic sample preparation

Before the characterization of samples, they were mounted in bakelite using the Struers[TM] Labopress-1 machine, which shown in Figure 4.19 (a). After that the specimens were polished on the Struers[TM] Tegrapol-15 automatic polishing machine which shown in Figure 4.19 (b). The aim of polishing process was preparing samples for XRD analysis, hardness test, fracture toughness evaluavation and SEM microstructure analysis.

4.3.2 Scanning Electron Microscopy (SEM)

SEM was used to investigate the microstructure of the zirconia specimens, which polished in metallography lab. Figure 4.20 shows JEOL[TM] JCM 6000 NeoScope scanning electron microscope equipped with a field emission gun operating between 5-15kV was used to analysis the microstructure of the polished specimens. The specimens were coated with gold using a gold-sputterer before being placed on the carbon tape and they were analyzed in magnification range of 500x-2000x. The

Energy Dispersive X-ray Spectrometer (EDS), which provided qualitative and quantitative analysis of elemental composition, is associated with SEM.

(a)   (b)

Figure 4.19 : (a) Struers^TM Labopress-1 machine, b) Struers^TM Tegrapol-15 automatic polishing machine.

Figure 4.20 : JEOL^TM JCM 6000 NeoScope scanning electron microscope.

4.3.3 X-ray diffraction (XRD) analysis

The Buruker^TM D8 Advanced Series Power Diffractometer, equipped with a copper anode using K_α as the radiation. The x-ray tube was operated at 35kV and 45 mA at a wavelength of 0.154 nm. The sccaning range was 10-90° (2Θ) using step size of 5°/min. Phase quantification was done using the Eva software.

Cubic and tetragonal phases are diffracted in very near 2Θ, which distinguished of them is difficult. Thus, their peaks were identified as t+c-ZrO_2 and other peaks were termed as m-ZrO_2.

Figure 4.21 : Buruker^{TM} D8 Advanced Series Power Diffractometer.

4.3.4 Particle size analysis

Raw materials particle size mesasurements were carried out in Malven^{TM} Mastersizer 2000 Laser particle size analyzer, which show in Figure 4.22. The analysis was done in water. Each powder was analysed three times and the average particle size was reported for it.

Figure 4.22 : Malven^{TM} Mastersizer 2000 Laser particle size analyzer.

4.3.5 Density and porosity measurements

The density and porosity of sintered samples were determined using Archimedes technique. First of all the dry mass was measured (m_d). According to TSE 4633 standard, samples were boiled in water for four hours in order to fill the pores. Then, the mass of the sample suspended in water was determined (m_s), followed by the water-saturated mass (m_w). The water-saturated mass was done by drying the surface of the sample with a paper towel then determining its mass. The mass measurements were done by Percisa^{TM} XB220A model sensitive balance. Density values were obtained from an average of five samples. The density and porosity was calculated using the equations 4.1 and 4.2 :

$$D = [m_d / (m_s - m_w)] \, \rho_{water} \tag{4.1}$$

$$\%\,Porosity = [(m_w - m_d)/(m_w - m_s)] \, 100 \tag{4.2}$$

where D is the bulk density (g/cm^3); m_d is the dry mass (g); m_s is the mass of the samples suspended in water (g); m_w is the water saturated mass (g); and ρ_{water} is the density of water (g/cm3); and Porosity is the percentage porosity.

Figure 4.23 : Percisa^{TM} XB220A model sensitive balance.

4.3.6 Hardness mesurement

Vickers hardness values were measured on polished surfaces at 0.5, 1 and 2 kg load held for ten seconds. The hardness values were obtained from an average of six indents on each of the two samples. Figure 4.24 shows Shimadzu^{TM} micro hardness tester.

Figure 4.24 : Shimadzu^{TM} micro hardness tester.

4.3.7 Three-point bending test

Measurement of flexural strength was performed using a three-point bending test in Shimadzu^{TM} AGS-J model instrument which shown in Figure 4.25. The distance between the supports was 30mm, the crosshead speed was 1mm/min and load at fracture was recorded. The flexural strength (σ_f) in mega Pascals (MPa) was calculated according to the following equation:

$$\sigma_f = 3PL/(2bd^2) \tag{4.3}$$

Figure 4.25 : ShimadzuTM AGS-J model 3.point bending test instrument.

where P is the load at fracture in Newtons (N), L the test span (centre-to-centre distance between the supporting rollers), b the width of the specimen, and d is the thickness of the specimen, all measured in millimetres (mm). Five specimens were tested at each type of samples.

4.3.8 Fracture toughness

The measurement of a ceramic's fracture toughness is not straight forward. A number of techniques may be employed which often lead to varying results. In this study, the fracture toughness of sintered samples was determined by "Vickers indentation" of Shimadzu^{TM} micro hardness tester, which shown in Figure 4.24. Vickers hardness pyramid indent was measured on polished surfaces at suitbale load held for ten seconds, then, the microcracks length was measured and the fracture toughness was obtained from the expression given by Evans. Y. Charles fracture toughness equation:

$$K_{IC} = 0.16 \ (c/a)^{-1.5}. \ (H_v.a^{0.5}) \tag{4.4}$$

where H_v is the Vickers hardness value, 2a the indentation diagonal and 2c the length of the full crack (both in micron).
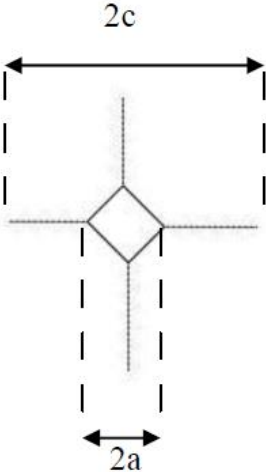

Figure 4.26 : Schematic of the Vickers hardness indentation.

5. RESULTS AND DISCUSSION

5.1 Particle Size Distribution

In this study, raw materials particle size and their distribution were measured by Malven^{TM} Mastersizer 2000 Laser particle size analyzer. Table 5.1 shows the powders particle size values of d(0.1), d(0.5), d(0.9).

Table 5.1 : Particle size distribution of raw materials.

Material	d(0.1)	d(0.5)	d(0.9)
	µm	µm	µm
Zirconia	4.58	8.25	14.57
Sintered MgO	1.51	2.77	5.74
TiO$_2$	0.52	1.24	2.91
Si$_3$N$_4$	4.07	24.34	57.8
SiC	0.74	2.44	5.85

5.2 Phase Analysis and X-ray Diffraction Data

Phase analysis of all specımens with different composıtion and sintering process were carried out by X-ray diffraction patterns. Cubic and tetragonal phases are diffracted in very near 2Ө, which distinguished of them is difficult. Thus, their peaks were identified as t+c-ZrO$_2$.

5.2.1 Monoclinic zirconia with addition of Si$_3$N$_4$

X-ray diffraction patterns of monoclinic zirconia samples (with 3.12 wt% MgO as stabilizer) with addition of 0, 5, 10 and 15 wt% Si$_3$N$_4$ are shown in Figure 5.1. Direct nitridation of ZrO$_2$ in a nitrogen atmosphere at temperatures between 1400 and 2200°C is formed oxygen-rich phase Zr$_7$O$_8$N$_4$ which has A$_7$X$_{12}$-type structure of Pr$_7$O$_{12}$ and presence of silicon nitride increase rate of this formation.

MgO in sample with 0 wt% silicon nitride was not performed its stabilizer role and monoclinic zirconia was main phase in the matrix. With increasing the content of Si$_3$N$_4$, both t+c ZrO$_2$ and Zr$_7$O$_8$N$_4$ phase were increased.
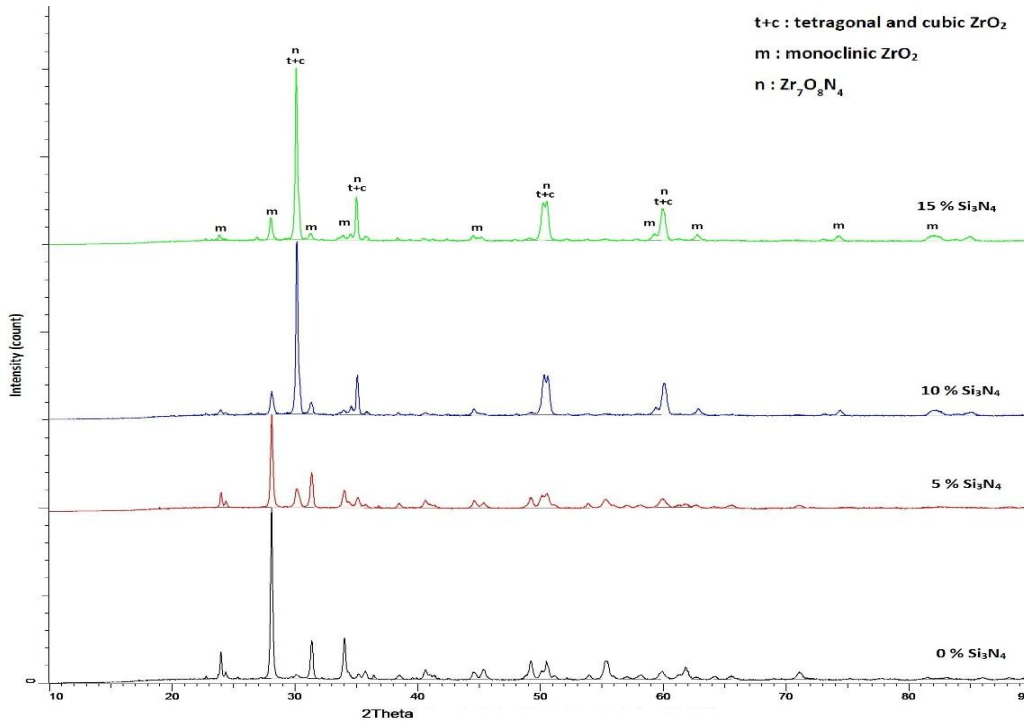
Figure 5.1 : X-ray patterns of monoclinic zirconia with Si_3N_4 samples.

5.2.2 Monoclinic zirconia (with MgO as stabilizer) with addition of TiO_2

5.2.2.1 Sinterd at 1400°C

Since sintering temperature and soaking time was too low, the peaks from tetragonal and cubic are not detected, thus, monoclinic phase is identified as major phase in all specimens. As seen in Figure 5.2 $Mg_2Zr_5O_{12}$ is formed just in sample containing 5 wt% TiO_2.

Magnesium zirconium titanium oxide phase is observed just in 10 and 15 wt% TiO_2 specimens. In 15 wt% TiO_2 portion of titanium dioxide was reacted with magnesium and formed $(MgTi_2)O_5$.

5.2.2.2 Sinterd at 1600°C and aged

As seen in Figure 5.3, t+c structure in 0 wt% TiO_2 sample perform main phase (about 70%), which it was occurred due to aging at 1100°C for 4 hours. Aging was allowed to tetragonal structure transformed to cubic phase, which has better mechanical properties. $Mg_2Zr_5O_{12}$ phase is not observed in specimen containing 5 wt% TiO_2 and it is very important in mechanical properties. With increasing TiO_2 content, tetragonal and cubic phase were reduced, where monoclinic phases

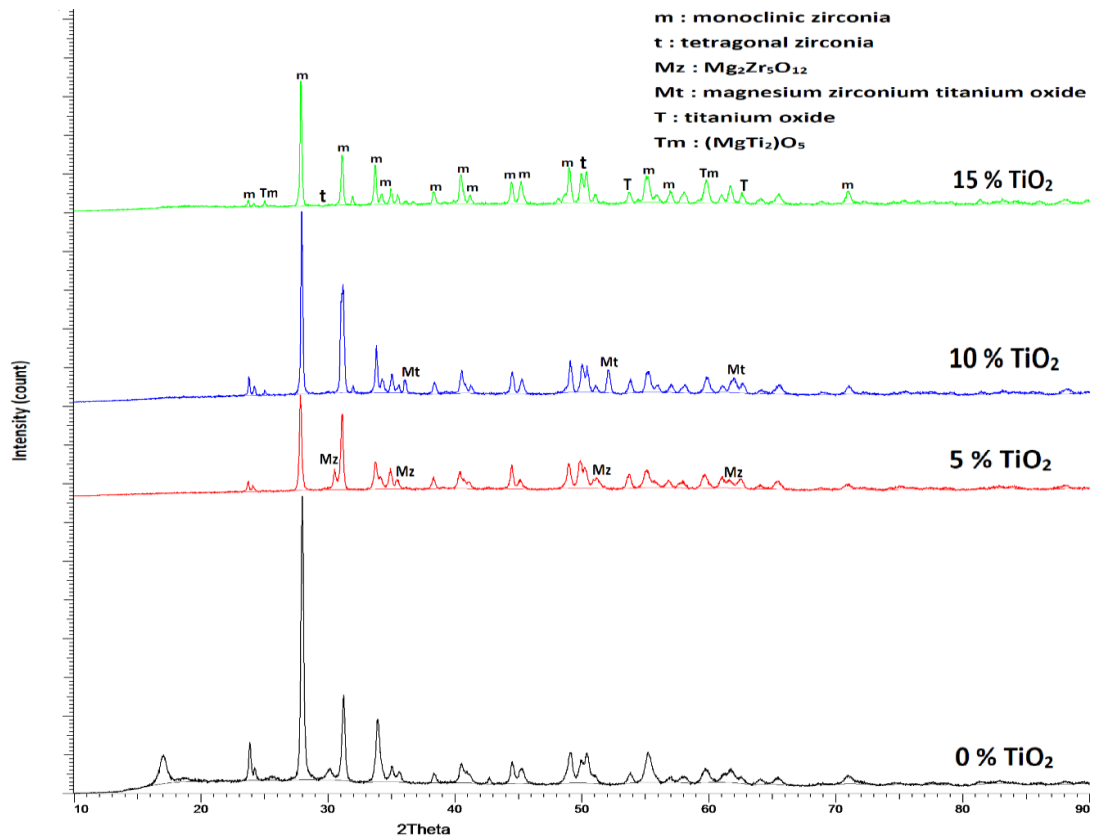increased. Magnesium zirconium titanium oxide phase is observed just in 10 and 15 wt% TiO_2 specimens.

Figure 5.2 : X-ray diffraction patterns of monoclinic zirconia with TiO_2 sintered at 1400°C.

5.2.3 Tetragonal stabilized zirconia with addition of TiO_2

5.2.3.1 Sinterd at 1400°C

It is evident from the Figure 5.4 that 0 wt% TiO_2 sample comprises primarily tetragonal and cubic phases, where monoclinic is as minor phase. In sample containing 5 wt% TiO_2, $Mg_2Zr_5O_{12}$ peaks are seen, also, monoclinic phase increases with increasing TiO_2 content.

Magnesium zirconium titanium oxide phase is observed just in 10 and 15 wt% TiO_2 specimens. In 15 wt% TiO_2 portion of titanium dioxide was reacted with magnesium and formed $(MgTi_2)O_5$.
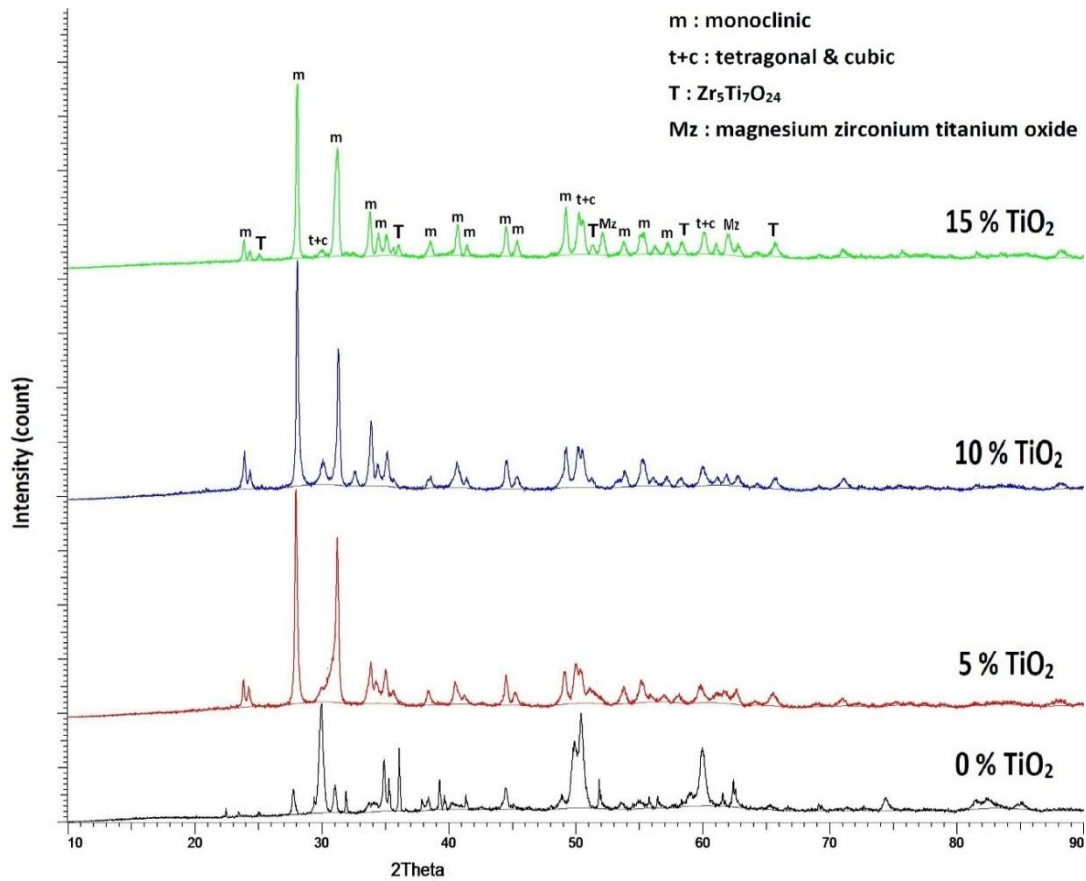
Figure 5.3 : X-ray diffraction patterns of monoclinic zirconia with TiO_2 sintered at 1600°C.

5.2.3.2 Sinterd at 1600°C and aged

Figure 5.5 shows X-ray diffraction patterns of as-sintered tetragonal stabilized zirconia with TiO_2 addition, which aged at 1100°C. 0 wt% TiO_2 sample is fully stabilized and it is formed only tetragonal and cubic phases.

In 5 wt% TiO2 some peaks can be indexed from $Mg_2Zr_5O_{12}$. Monoclinic phase increases with increasing TiO_2 content. Magnesium zirconium titanium oxide phase is observed just in 10 and 15 wt% TiO_2 specimen.
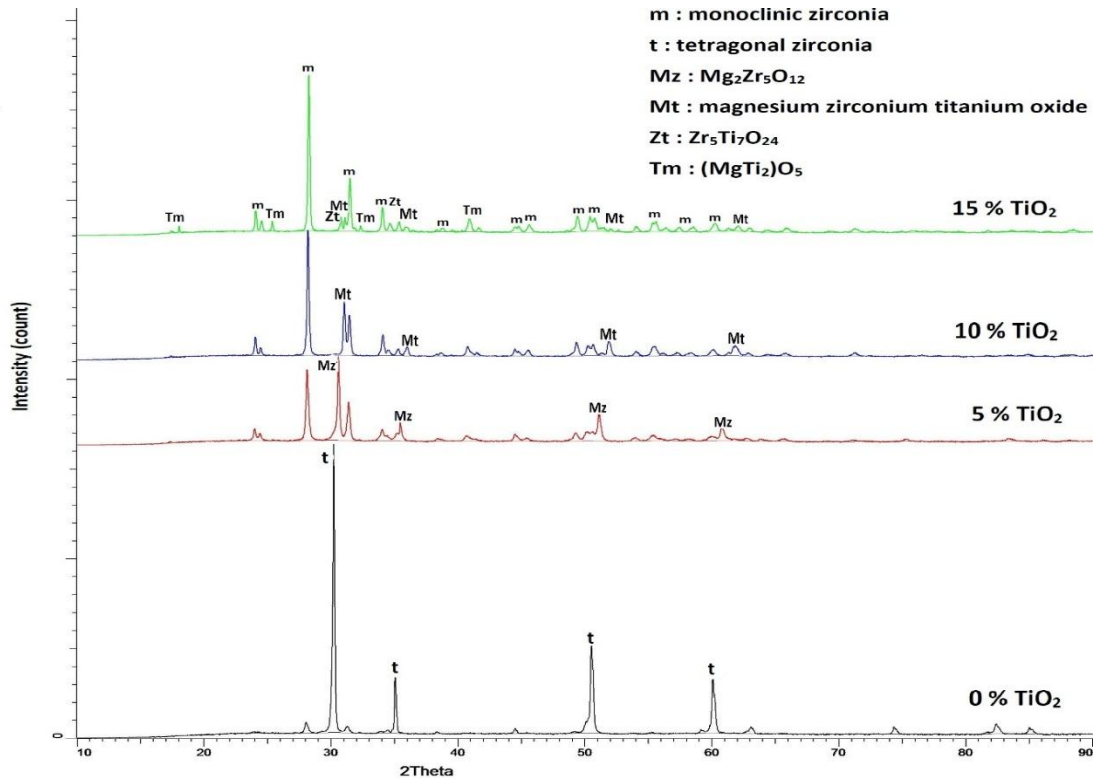
Figure 5.4 : X-ray diffraction patterns of stabilized zirconia with TiO_2 sintered at 1400°C.
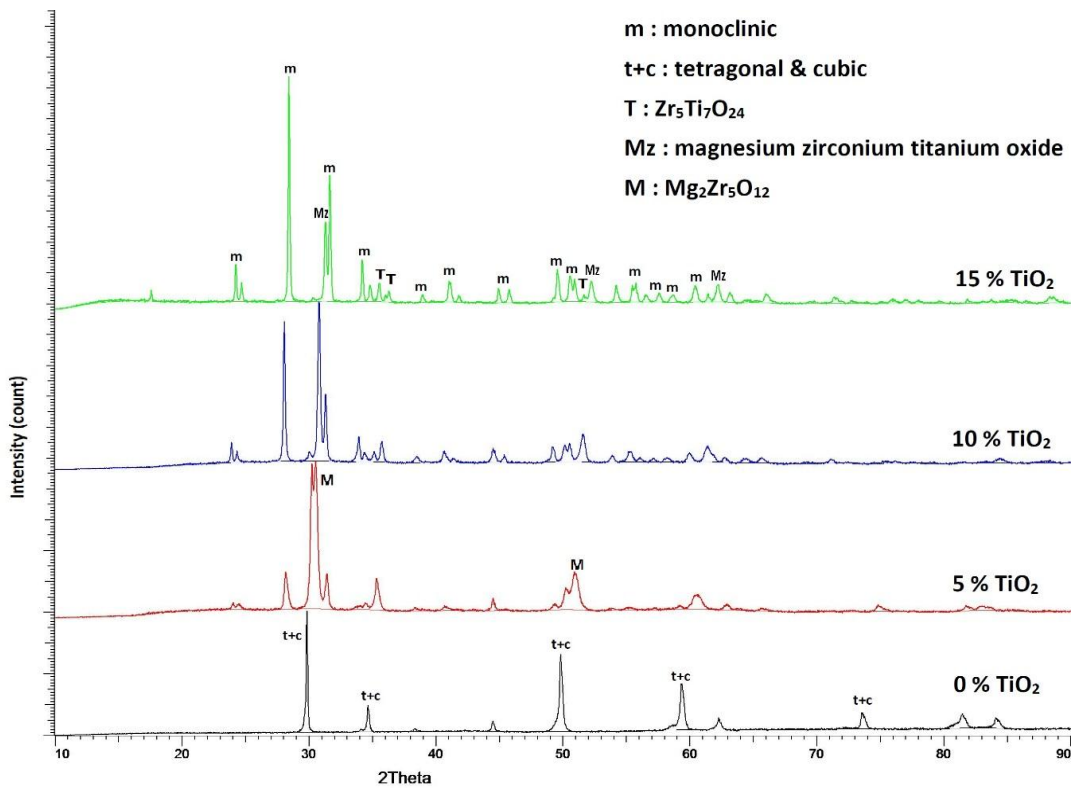

Figure 5.5 : X-ray diffraction patterns of stabilized zirconia with TiO_2 sintered at 1400°C.

5.3 Scanning Electro Microscopy (SEM)

Sintered samples were prepared by polishing in metallography lab. Scanning electron microscope equipped with a field emission gun operating between 5-15kV was used to analysis the microstructure.
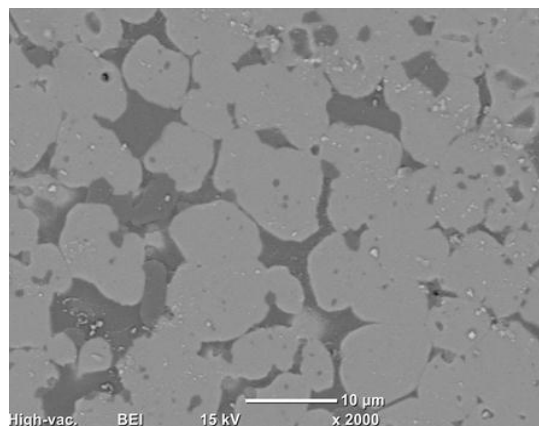
5.3.1 Monoclinic zirconia with addition of Si_3N_4

Figure 5.6 illustrates an example of the SEM micrograph in the as-sintered zirconia containing Si_3N_4. Grain sizes of specimens were increased with increasing content of Si_3N_4, on the other hand grain boundries in 5 wt% Si_3N_4 are very porous, however, they are filled by liquid phase in 15 wt% Si_3N_4.
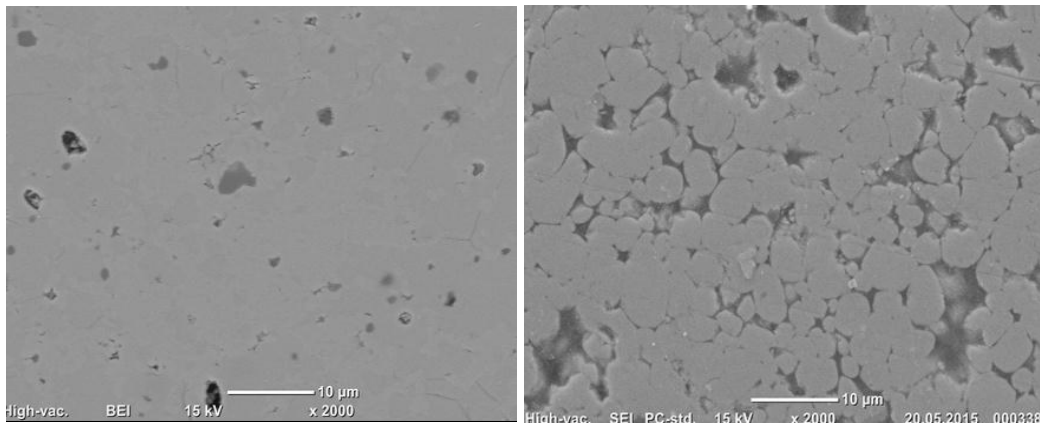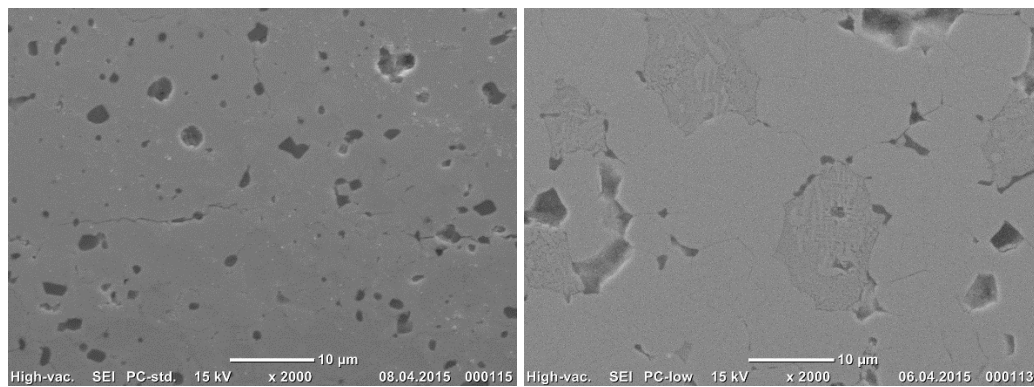

(a)   (b)

(c)

Figure 5.6 : SEM micrograph of monoclinic zirconia with addition of Si_3N_4 sintered at 1600°C (a) 0 wt% Si_3N_4 (b) 5 wt% Si_3N_4 (c) 15 wt% Si_3N_4.

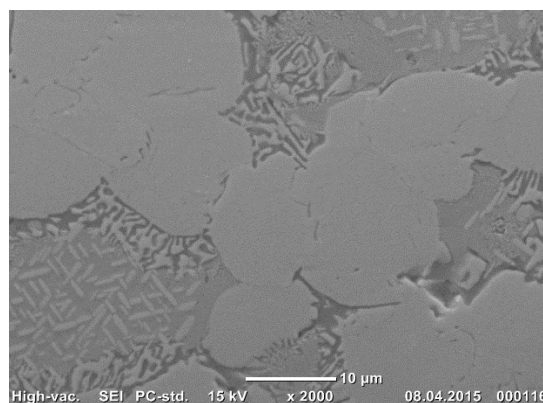### 5.3.2 Monoclinic zirconia with addition of TiO₂

SEM analysis of different specimens of monoclinic zirconia (MgO as stabilizer) with addition of TiO_2, which sintered at 1600°C and aged at 1100°C are shown in Figure 5.7. The sample containing 0 wt% TiO_2 (Figure 5.7 a) presents a homogeneous morphology comprised monocilinic, tetragonal and cubic phases as abtained by XRD patterns.

In 5 wt% TiO_2, two different kind of structure were evidenced (Figure 5.7 b). Matrix with homogeneous grain, which can be formed monoclinic structure, also Mg and Ti amount is very low. On the other hand, Mg and Ti-rich grains is observed, where needle-shape tetragonal zirconia are distributed among the grains. However, these tetragonal precipitates are too large and their effect on mechanical properties is disappear.

(a) (b)

(c)

Figure 5.7 : SEM micrograph of monoclinic zirconia with addition of TiO_2 sintered at 1600°C (a) 0 wt% TiO_2 (b) 5 wt% TiO_2 (c) 15 wt% TiO_2.

In 15 wt% TiO_2 (Figure 5.7c), likewise previous sample two different type of grains are obtained, however, the grain size in it is larger than other samples due to presence of high amount of TiO_2, which led to grain growth.

5.3.3 Tetragonal stabilized zirconia with addition of TiO_2

Figure 5.8 shows the SEM micrograph of tetragonal stabilized zirconia with addition of TiO_2 sintered at 1600°C, in which the grians size are increased with increasing content of TiO_2. In the specimen containing 5 wt% TiO_2 (Figure 5.8 b) similar to monoclinic zirconia with 5 wt% TiO_2, there are two different kinds of morphology: matrix and needle-shaped tetragonal structure. However, here amount of Mg and Ti are higher in needle-shaped structure. The present results suggest that the addition of TiO_2 to tetragonal stabilized zirconia gives rise to the concentration of $Mg_2Zr_5O_{12}$ which observed by XRD Pstterns.

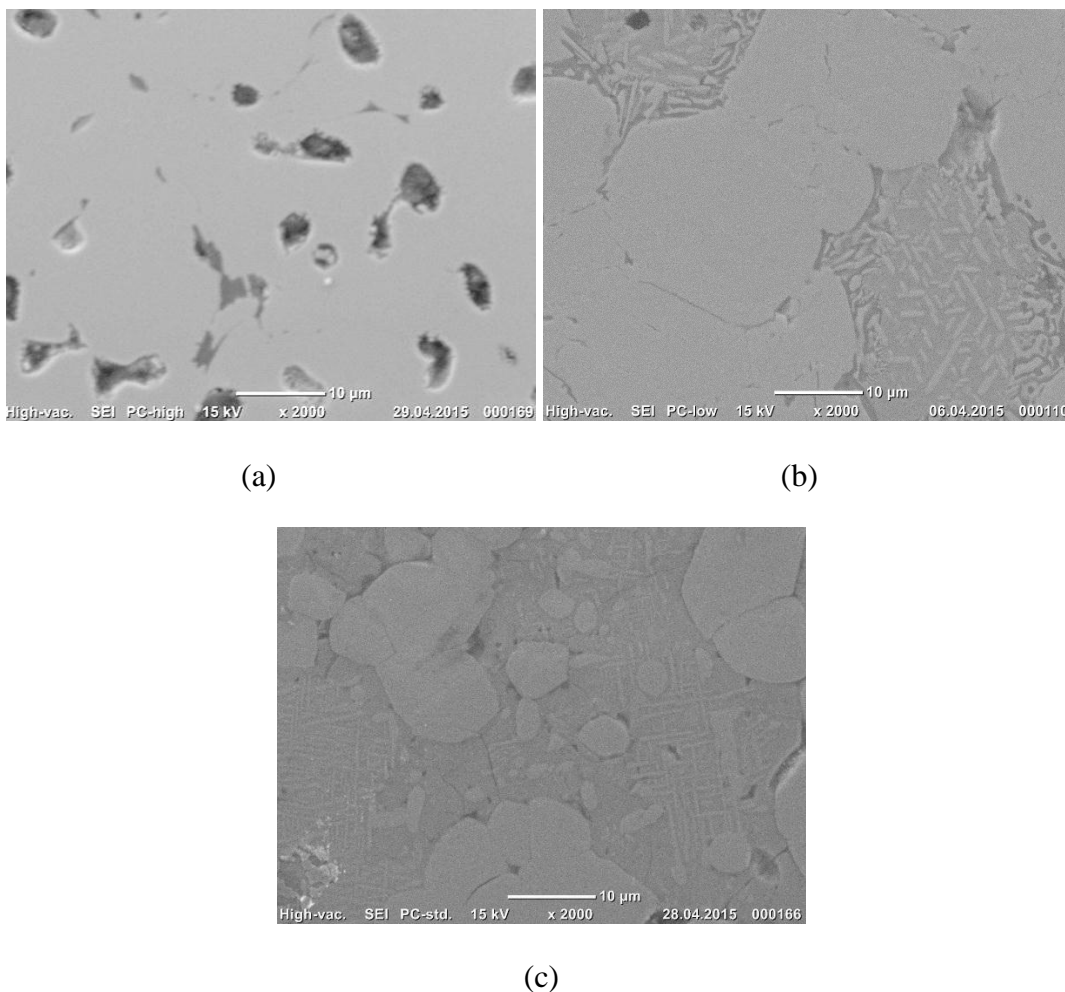(a)   (b)

(c)

Figure 5.8 : SEM micrograph of tetragonal stabilized zirconia with addition of TiO_2 sintered at 1600°C (a) 0 wt% TiO_2 (b) 5 wt% TiO_2 (c) 10 wt% TiO_2.

In 10% TiO_2 specimen (Figure 5.8c) needle-shpaed grians are increased by increasing TiO_2, also results are shown Mg and Ti rich phase were distributed all over the sample.

5.4 Density and Porosity Measurment

The density and porosity of as-sintered specimens were determined using Archimedes technique. Density values were obtained from an average of five samples. The density and porosity was calculated using the equations 5.1 and 5.2 :

$$D = [m_d / (m_s - m_w)] \, \rho_{water} \qquad (5.1)$$

$$\%Porosity = [(m_w - m_d)/(m_w - m_s)] \, 100 \qquad (5.2)$$

where D is the bulk density (g/cm^3); m_d is the dry mass (g); m_s is the mass of the samples suspended in water (g); m_w is the water saturated mass (g); and ρ_{water} is the density ofwater (g/cm^3); and Porosity is the percentage porosity.
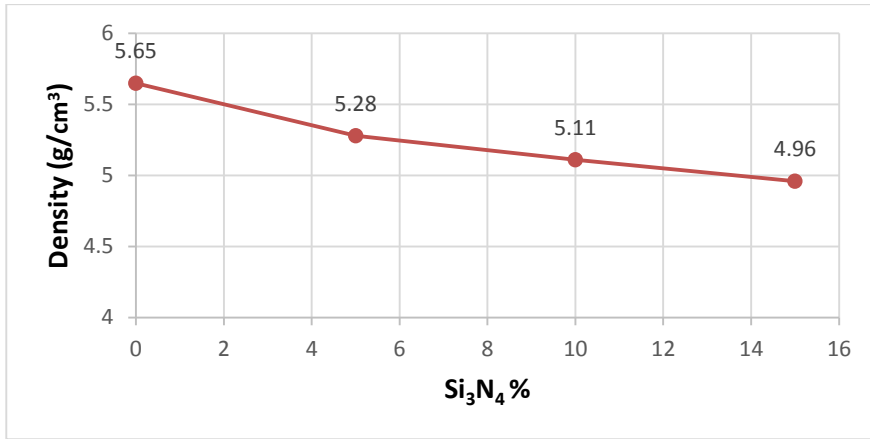
5.4.1 Monoclinic zirconia with addition of Si_3N_4

Bulk density and apparent porosity of as-sintered samples are shown in Figure 5.9 (a) and (b). The values of density are 5.65, 5.28, 5.11, 4.96 g/cm^3 for 0, 5, 10, 15 wt% Si_3N_4, respectively. Also, percentage of theorical densities are 98, 93.6, 92.5, 91.8 %, respectively. Decreasing densification of silicon nitride containing samples can be related to low density of Si_3N_4 powder.

Acording to SEM micrographs, inter-granular porosities are high in 5 wt% Si_3N_4, which liquid phase was filled these porosies in higher content of Si_3N_4. Therefore, apparent porosity of 5 wt% Si_3N_4 is higher than other specimens.

5.4.2 Monoclinic zirconia with addition of TiO_2

Figure 5.10 (a) and (b) shows bulk density and apparent porosity values of specimens which sintered at 1400°C. The bulk density values are 5.57, 5.39, 5.22, 4.98 g/cm^3 and percentage of theorical density are 96.7, 95, 93.4, 90.4 % for 0, 5, 10, 15 wt% TiO_2, respectively.
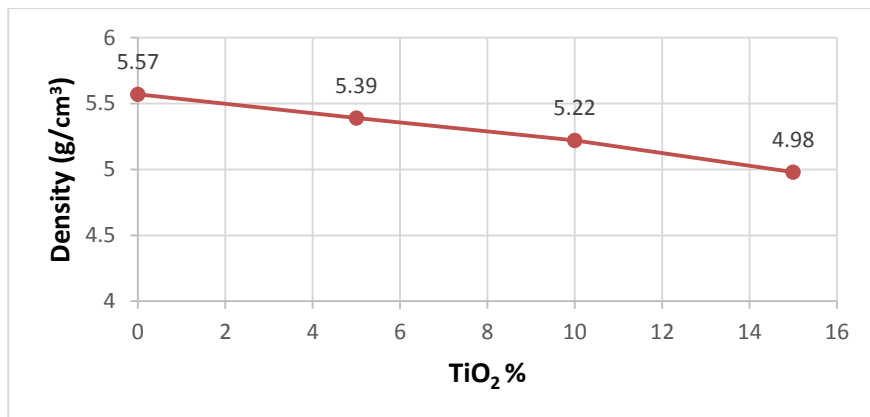
(a)
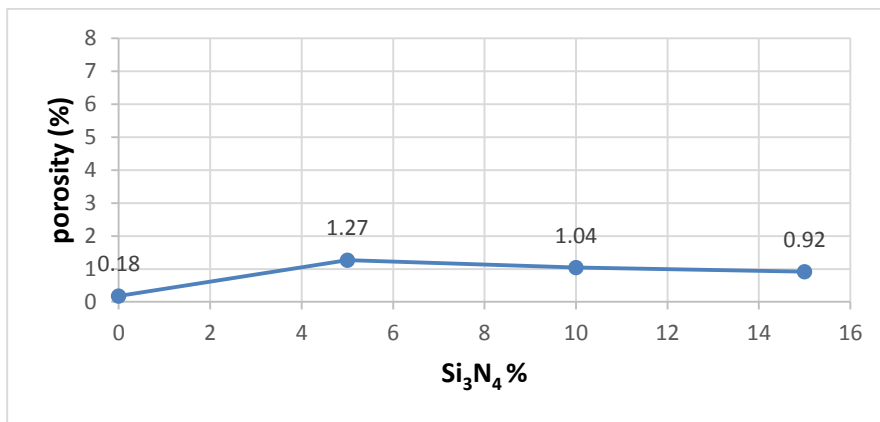
(b)

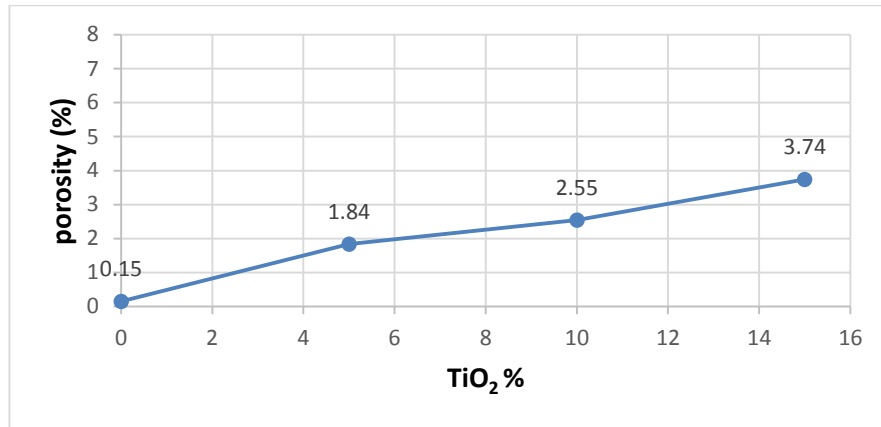**Figure 5.9 :** (a) Density , (b) Apparent Porosity of Monoclinic zirconia with addition of Si_3N_4.

Figure 5.11 (a) and (b), illustrates the results of bulk density and apparent porosity of samples sintered at 1600°C and aged. The bulk density values are 5.5, 5.18, 4.9, 4.88 g/cm^3 and percentage of theorical density are 95.5, 91.3, 87.6, 88.6 % for 0, 5, 10, 15 wt% TiO_2, respectively.
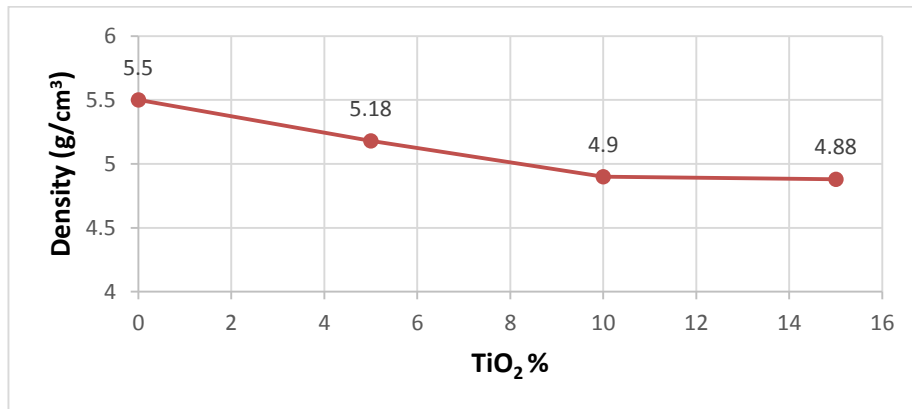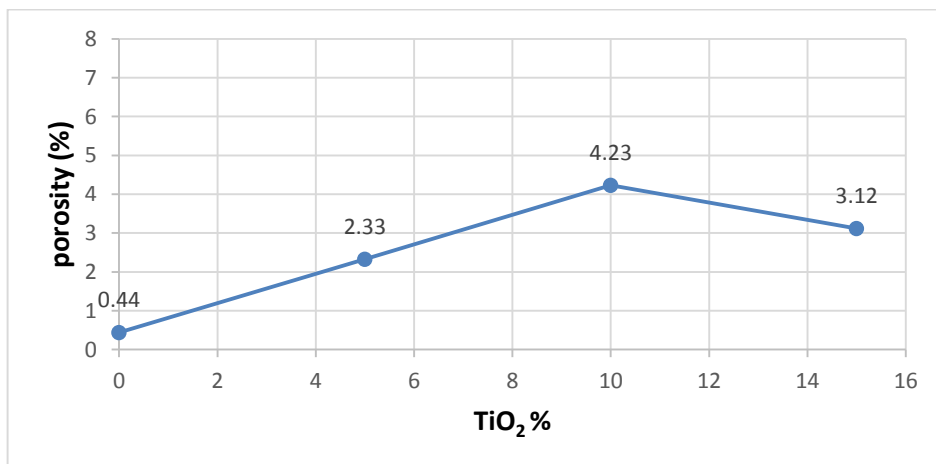
(a)

(b)

Figure 5.10 : (a) Density , (b) Apparent Porosity of Monoclinic zirconia with addition of TiO$_2$ sintered at 1400°C.


(a)

(b)

Figure 5.11 : (a) Density , (b) Apparent Porosity of Monoclinic zirconia with addition of TiO$_2$ sintered at 1600°C.

It can be seen from these figures that the as-sintered density of the specimens decreased with increasing TiO_2 content. This decreased density with increasing TiO_2 content could be due to the grain growth and a small amount of intergranular porosity formed in the grain interior and along the grain boundaries. The SEM micrographs are showed that the grain size increased with increasing TiO_2 content. Apparent porosity enhancement is evidence for increasing porosity between grains.

5.4.3 Tetragonal stabilized zirconia with addition of TiO_2

Bulk density and apparent porosity results of samples sintered at 1400°C are shown in Figure 5.12 (a) and (b). The values of density are 4.23, 5.19, 5.24, 5.08 g/cm^3 for 0, 5, 10, 15 wt% TiO_2, respectively. Also, percentage of theorical densities are 69.6, 86.8, 89.1, 87.6 %, respectively
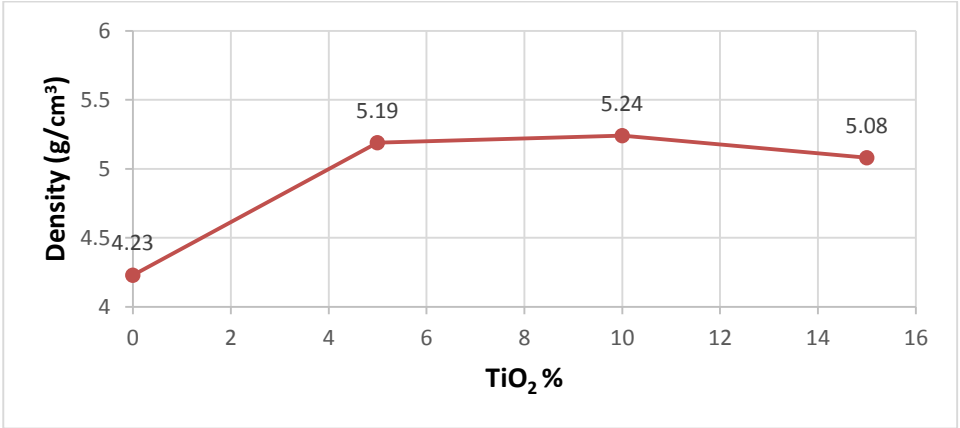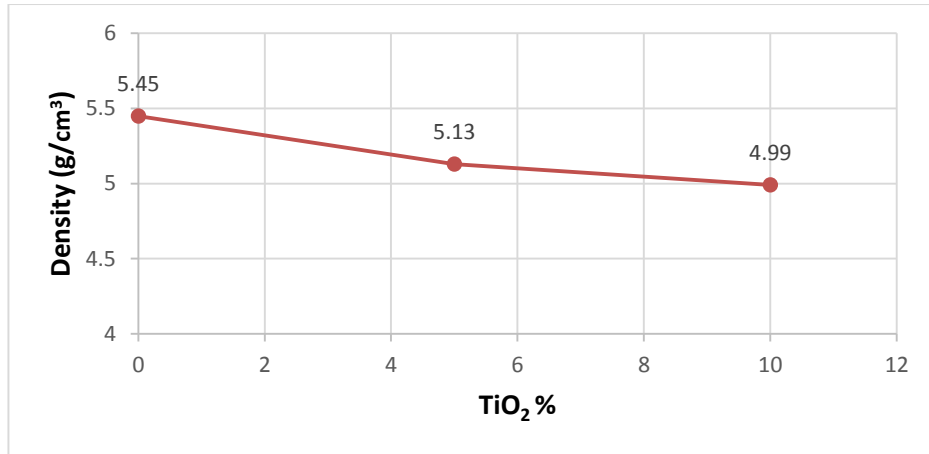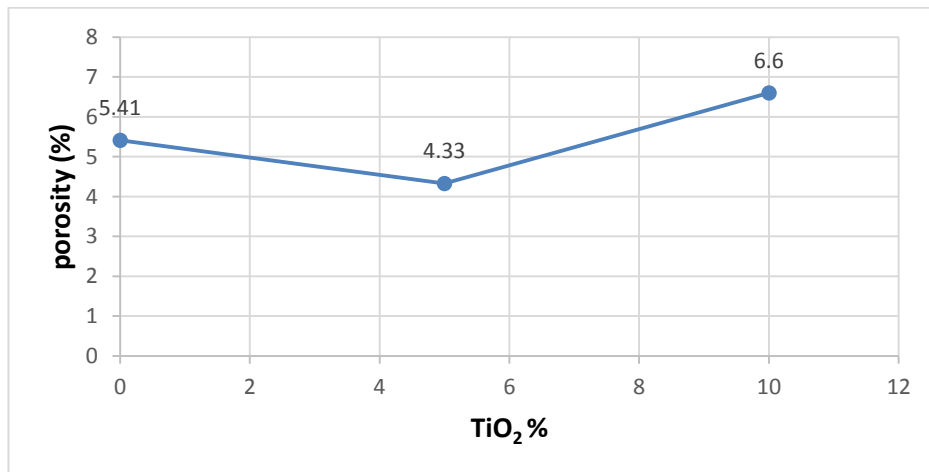

(a)
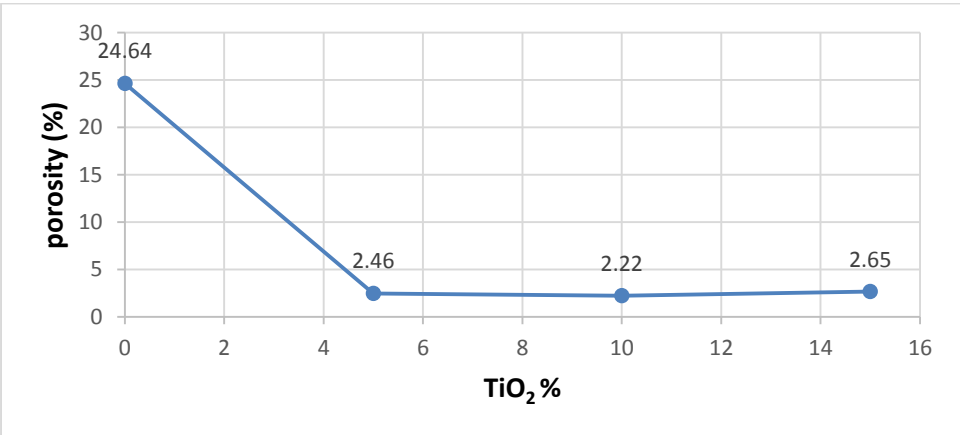
(b)

Figure 5.12 : (a) Density , (b) Apparent Porosity of tetragonal stabilized zirconia with addition of TiO_2 sintered at 1400°C.

Figure 5.13 (a) and (b), shows bulk density and apparent porosity result of samples sintered at 1600°C and aged. The bulk density values are 5.45, 5.13, 4.99 g/cm^3 and percentage of theorical density are 89.63, 85.8, 84.71 % for 0, 5, 10 wt% TiO$_2$, respectively.

(a)

(b)

Figure 5.13 : (a) Density , (b) Apparent Porosity of tetragonal stabilized zirconia with addition of TiO$_2$ sintered at 1600°C.

In sample containing 0 wt% TiO$_2$ sintered at 1400°C, densification was not occurred compeletly because of low sintering temperature and soaking time. Also SEM micrograph of this specimen was showed very porous structure. As seen in Figure 5.12 (b) partancege of porosity for it is higher than other samples. Addition of TiO$_2$ can be developed sintering process by formation liquid phase. Thus, density was enhanced for samples containing TiO$_2$, however, the slow grain growth at low temperature was not provided condition for increasing porosity.

In specimens sintered at 1600°C for 5 hours and aged, increasing TiO_2 was led to grain growth and formation porosity between grains. Thus, with increasing TiO_2 content, density value decreases.

5.5 Mechanical Properties

During sintering, tetragonal stabilized zirconia with addition of 15 wt% TiO_2 which sintered at 1600°C was failed due to some phase transition and mechanical test was not crried out for it.

Figure 5.14 : Tetragonal stabilized zirconia with addition of 15 wt% TiO_2 sintered at 1600°C.

5.5.1 Hardness

5.5.1.1 Monoclinic zirconia with addition of Si_3N_4

Figure 5.15 illustrates the hardness values specimens sintered at 1600°C as a function of Si_3N_4 content. It can be seen from the figure that the hardness of the specimens decreased with increasing Si_3N_4 content up to 5 wt% and further increases in Si_3N_4 content led to an increase in hardness.

Table 5.2 : Hardness values of monoclinic zirconia with addition of Si_3N_4.

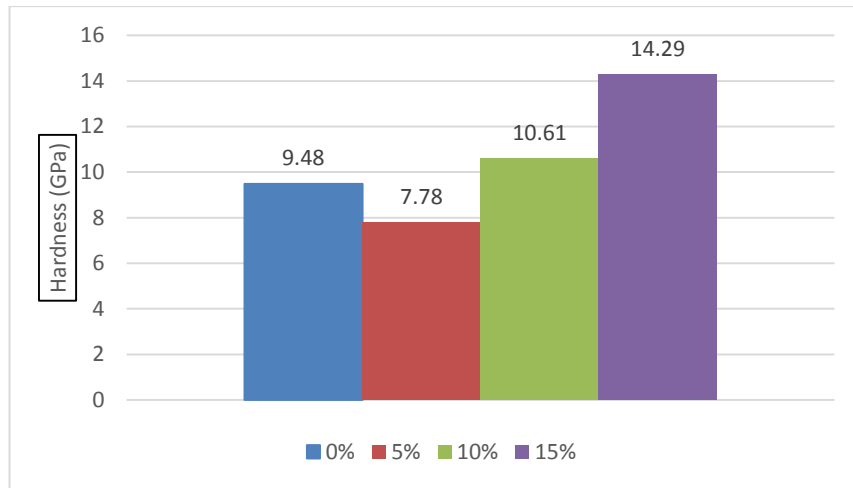| Si_3N_4%	0	5	10	15
Hardness (HV kg/mm^2)	966.8±79.2	793.87±53.87	1081.6±105.3	1457.7±74.2
Hardness (GPa)	9.48±0.77	7.78±0.52	10.61±1.03	14.29±0.72

Figure 5.15 : Hardness values of monoclinic zirconia with addition of Si_3N_4 graph.

In general, it is known that porosity in a ceramic material directly affect the values of hardness, where hardness decreses with porosity. In silicon nitride containing specimens, porostiy was increased up to 5 wt% Si_3N_4, then reduced with increasing Si_3N_4 content, and hardness values fit porosity. Also, in 5 wt% Si_3N_4 specimen porosities was formed inter-granulary, thus, highest apperent porosity amount can be seen in this specimen.

5.5.2 Monoclinic zirconia with addition of TiO_2

Figure 5.16 shows hardness values of monoclinic zirconia with addition of TiO_2 sintered at 1400°C. It was seen that the addition of TiO_2 reduced the hardness of the specimens and the hardness decreased from 7.71 to 3.53 GPa with an increase of TiO_2 content.

Table 5.3 : Hardness values of monoclinic zirconia with addition of TiO_2 sintered at 1400°C.

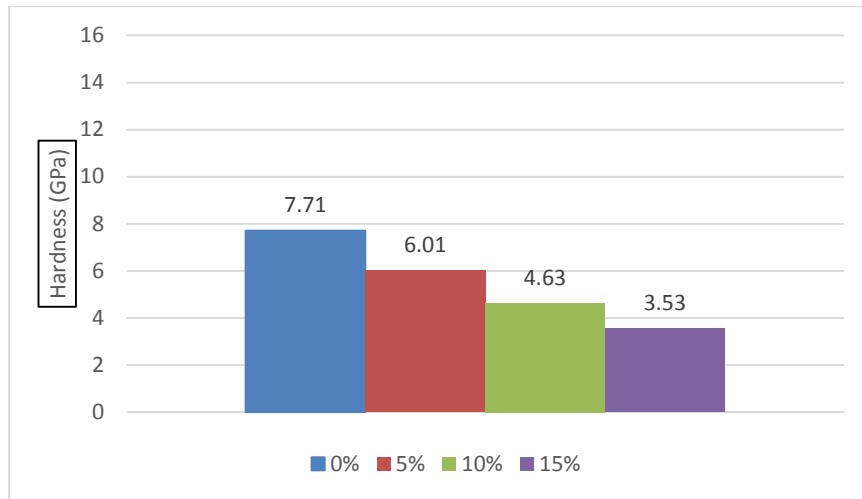| TiO_2%	0	5	10	15
Hardness (HV kg/mm²)	787.53±53	612.85±41.85	472.83±36.83	360.6±40.6
Hardness (GPa)	7.71±0.51	6.01±0.41	4.63±0.36	3.53±0.39

Figure 5.16 : Hardness values of monoclinic zirconia with addition of TiO_2 sintered at 1400°C graph.

Figure 5.17 shows hardness values of monoclinic zirconia with addition of TiO_2 sintered at 1600°C. Hardness value of specimens are decreased with increasing TiO_2 content from 7.76 to 3.5 GPa.

Table 5.4 : Hardness values of monoclinic zirconia with addition of TiO_2 sintered at 1600°C.

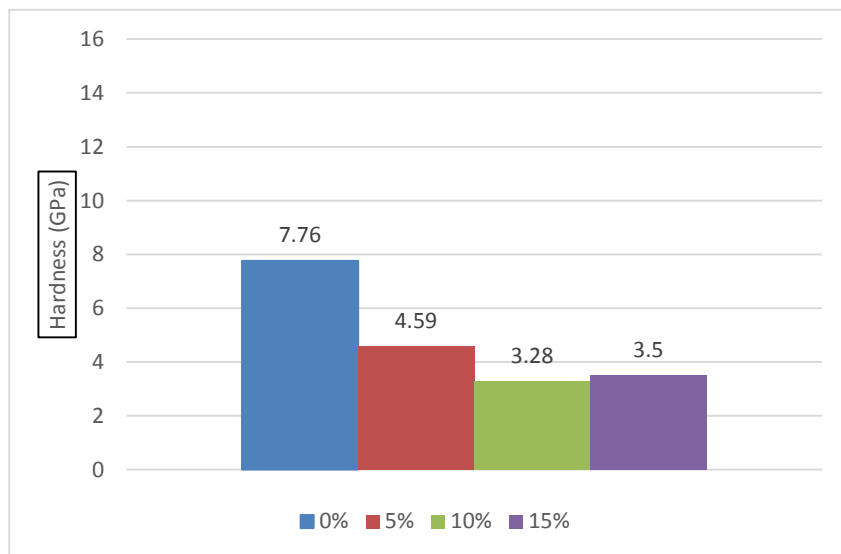| TiO_2%	0	5	10	15
Hardness (HV kg/mm^2)	791.57±51.5	468.5±32.4	334.6±39.6	357.66±53.4
Hardness (GPa)	7.76±0.5	4.59±0.31	3.28±0.38	3.5±0.52

Figure 5.17 : Hardness values of monoclinic zirconia with addition of TiO_2 sintered at 1600°C graph.

As mentioned above, hardness reduces with increasing porosity. Acourding to porosity results of monclinic zirconia with addtion TiO_2, hardness was increased with increasing TiO_2 content similar to porosity.

5.5.3 Tetragonal stabilized zirconia with addtion of TiO_2

Figure 5.18 illustrates the results of hardness of tetragonal stabilized zirconia sintered at 1400°C as a function of TiO_2 content. It can be seen from the figure that the hardness of the specimens enhencend with increasing TiO_2 content up to 5 wt% and further increase in TiO_2 content led to an decrease in hardness. This behavior can be explained by porosity graph was shown in Figure 5.12 (b). It is seen porosity has a minimum in 5 wt% Si_3N_4 and 0 wt% Si_3N_4 specimen present high amount of porosity. it is known that porosity increased hardness of ceramic materials.

Table 5.5 : Hardness values of tetragonal stabilized zirconia with addition of TiO_2 sintered at 1400°C.

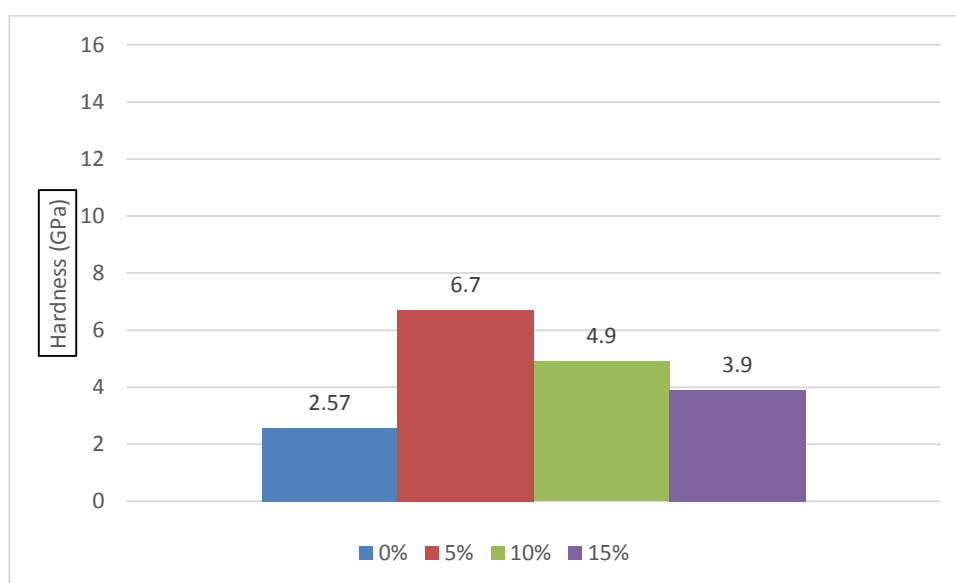| TiO_2%	0	5	10	15
Hardness (HV kg/mm^2)	262.66±25.6	683.33±56.6	500.28±52.8	398.28±47.2
Hardness (GPa)	2.57±0.25	6.7±0.55	4.90±0.51	3.9±0.46

Figure 5.18 : Hardness values of tetragonal stabilized zirconia with addition of TiO_2 sintered at 1400°C graph.

Hardness results of tetragonal stabilized zirconia with addition of TiO_2 sintered at 1600°C is shown in Figure 5.19. It was seen that the addition of TiO_2 increased the hardness of the specimens and the hardness decreased from 7.47 to 2.91 GPa with an increase of TiO_2 content. Similir to other samples, porosity effect on hardness results.

Table 5.6 : Hardness values of tetragonal stabilized zirconia with addition of TiO_2 sintered at 1600°C.

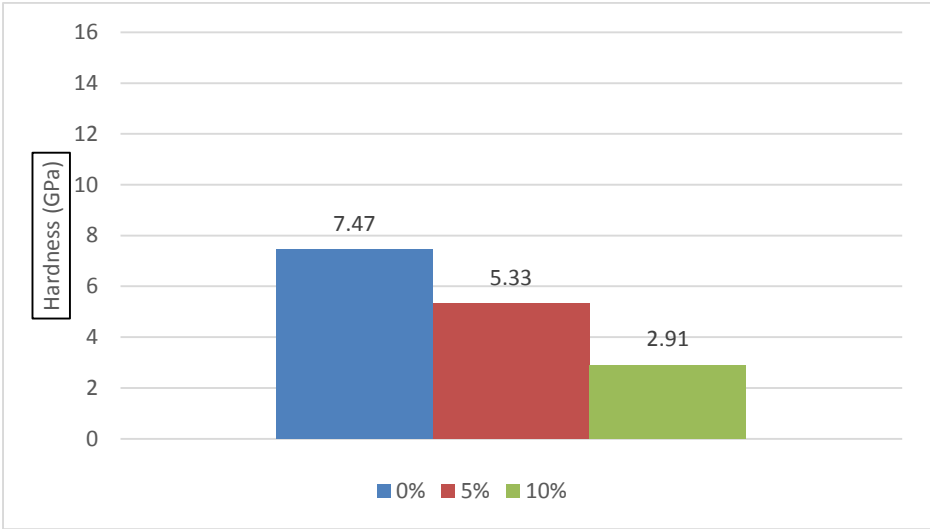| TiO_2%	0	5	10	15
Hardness (HV kg/mm^2)	761.84±48.1	543.66±59.3	297±56	-
Hardness (GPa)	7.47±0.47	5.33±0.58	2.91±0.54	-

Figure 5.19 : Hardness values of tetragonal stabilized zirconia with addition of TiO_2 sintered at 1600°C graph.

5.5.4 Bending test and fracture toughness

In general, it is known that strength and fracture toughness increase with a decrease in either porosity or grain size, however, low porosity is obtained usually only at the expense of considerable grain growth. Therefore the fabrication of high strength specimens depends on achieving the optimum balance between decreasing porosity and grain size.

5.5.4.1 Monoclinic zirconia with addition of Si_3N_4
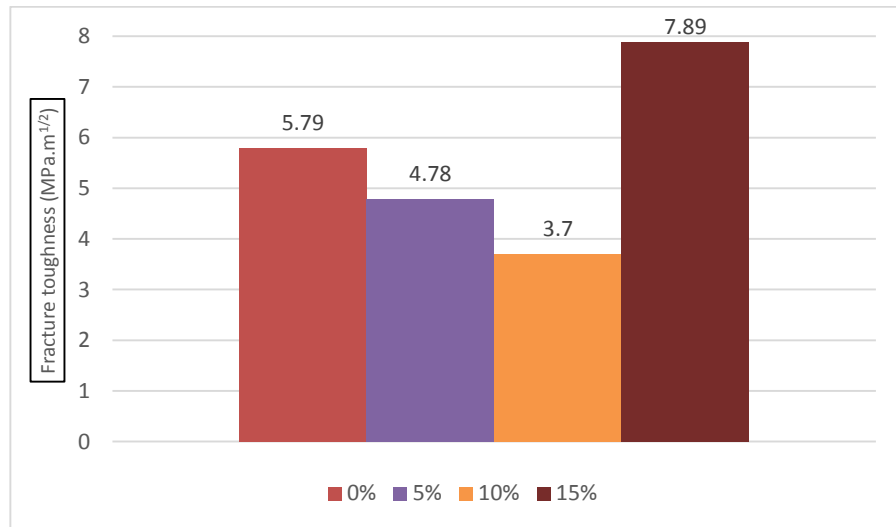
Figure 5.20 illustrates the results of flexural strength and fracture toughness of monoclinic zirconia as a function of Si_3N_4 content. The strength value was decresed up to 5 wt% Si_3N_4 then increased to 134 MPa in 15 wt% Si_3N_4.
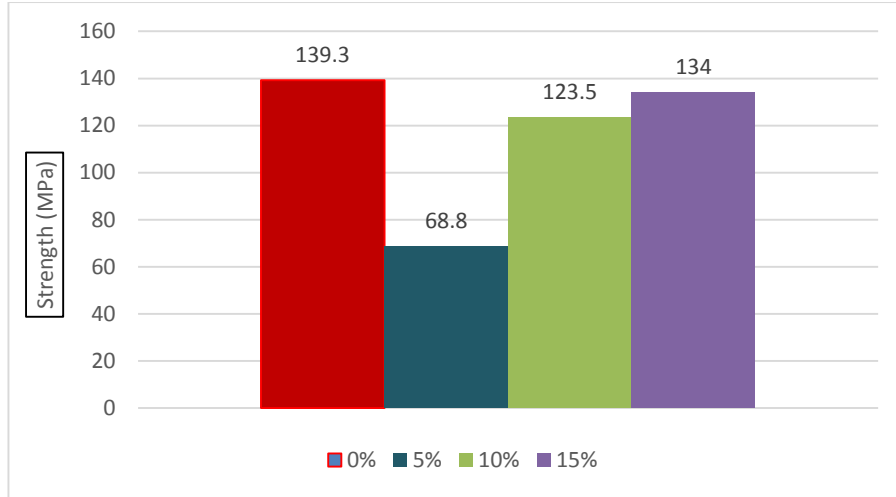
(a)

(b)

Figure 5.20 : (a) Flexural strength (b) Fracture toughness values of monoclinic zirconia with addition of Si_3N_4 graphs.

The measured toughness values increased with increasing Si_3N_4 content. The highest value of toughness, 7.89 MPa·m$^{1/2}$ was observed in the case of zirconia sample which contain 15 wt% of silicon nitride. As mentioned before in this specimen liquid phase was formed while sintering process and filled the porosites, thus, mechanical properties of specimen were improved.

5.5.4.2 Monoclinic zirconia with addition of TiO$_2$

Three point bending test and fracture toughness results for monoclinic zirconia sintered at 1400 and 1600°C are shown in Figure 5.21 and Figure 5.22 respectively. Unlike specimens sintered at 1600°C, which strength reduced by adding TiO$_2$, in 1400°C sintered samples addition of TiO$_2$ improved flexural strength and the higest value is 115.6 MPa for 5 wt% TiO$_2$. In this specimen presence of tetragonal precipitates and Mg$_2$Zr$_5$O$_{12}$ increase both strength and fracture toughness values which are not appear in other specimens.
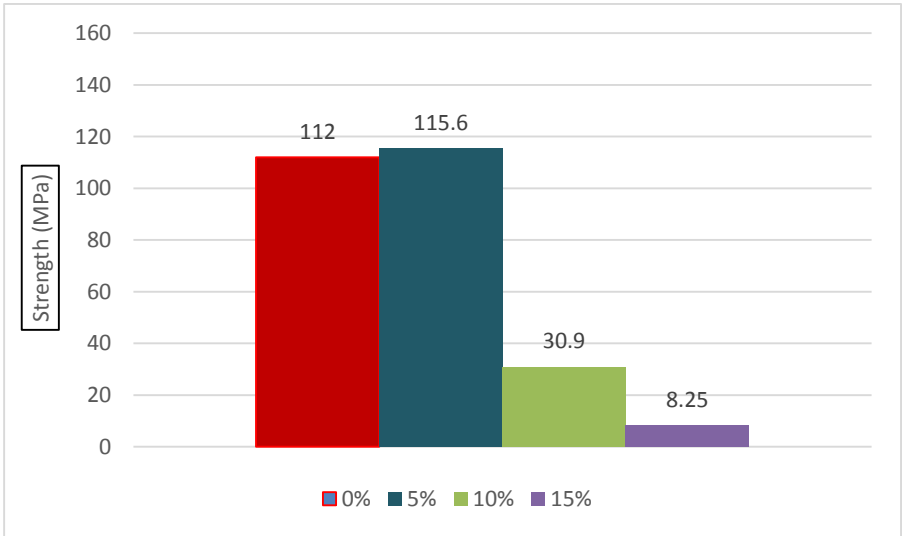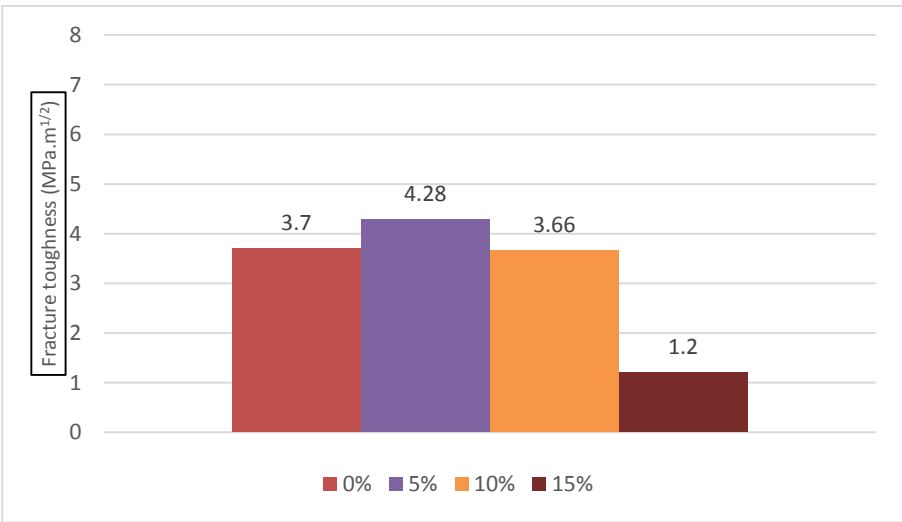

(a)

(b)

Figure 5.21 : (a) Flexural strength (b) Fracture toughness values of monoclinic zirconia with addition of TiO$_2$ sintered at 1400°C graphs.

Increasing sintering temperature up to 1600°C leads to grain growth and strength and fracture toughness are reduced. Therefore, better mechanical properties are obtained in lower sintering temparture in monoclinic specimens containing TiO_2.
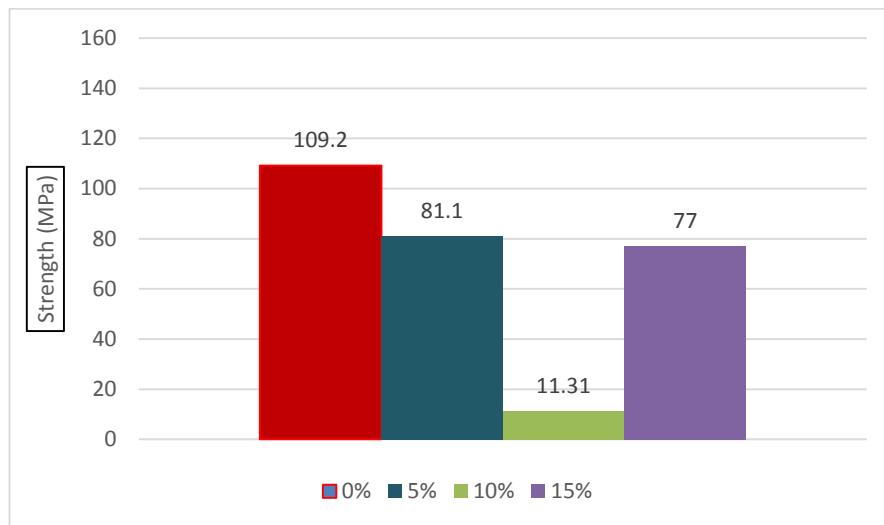

(a)
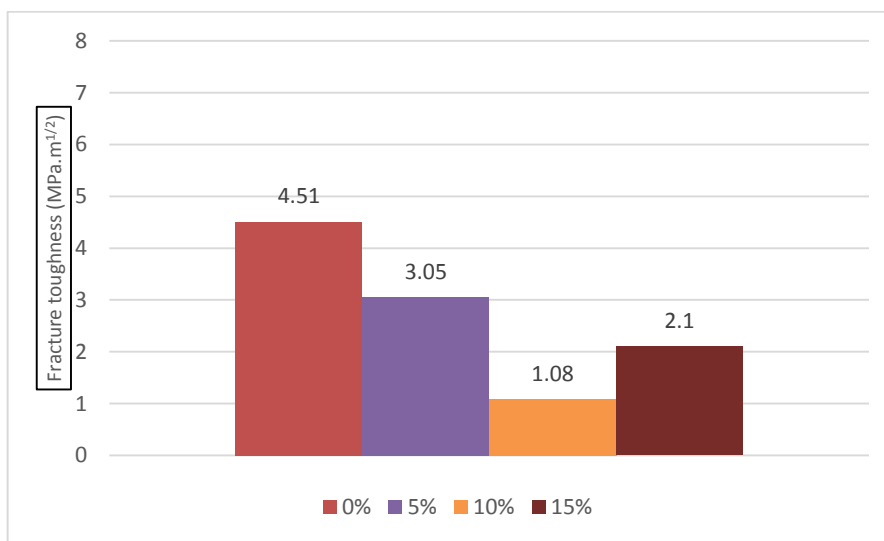
(b)

Figure 5.22 : (a) Flexural strength (b) Fracture toughness values of monoclinic zirconia with addition of TiO_2 sintered at 1600°C graphs.

5.5.4.3 Tetragonal stabilized zirconia with addition of TiO_2

Figure 5.23 and Figure 5.24 demonstrate the results of flexural strength and fracture toughness values of tetragonal stabilized zirconia sintered at 1400°C and 1600°C as a function of TiO_2 content, repectively.
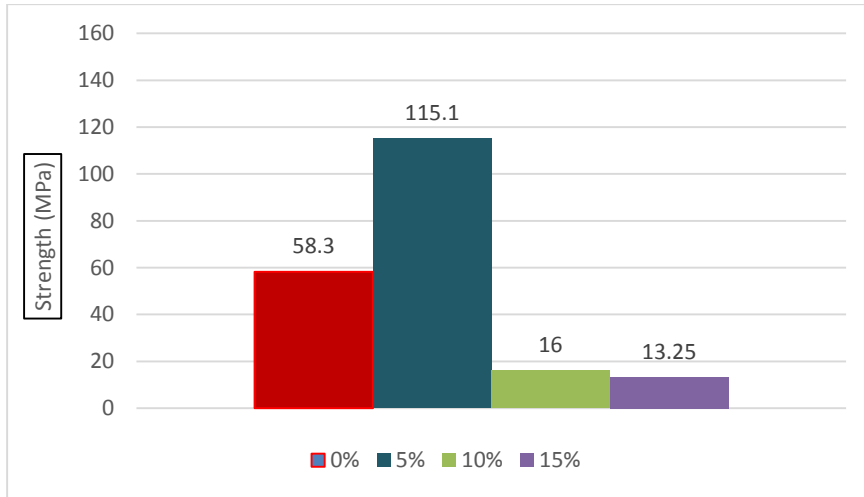
(a)
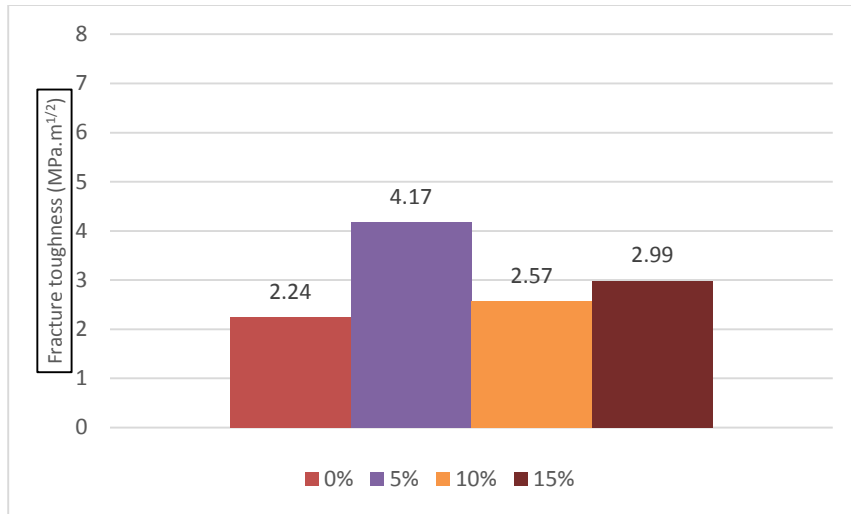
(b)

Figure 5.23 : (a) Flexural strength (b) Fracture toughness values of tetragonal stabilized zirconia with addition of TiO_2 sintered at 1400°C graph.

Likewise monoclinic zirconia specimens, in 1400°C sintered samples addition of TiO_2 improved flexural strength and the higest value is 115.1 MPa for 5 wt% TiO_2. In this specimen presence of tetragonal precipitates and $Mg_2Zr_5O_{12}$ increase both strength and fracture toughness values which are not appear in other specimens.

Results revealed that adding TiO_2 to zirconia, was improved mechanical properties and high temperature sintering and ageing are not necessary. Furthermore increasing amount of TiO_2 more than 5 wt% was removed useful mechanical properties because of formation of some Ti and Mg-rich phases while sintering.
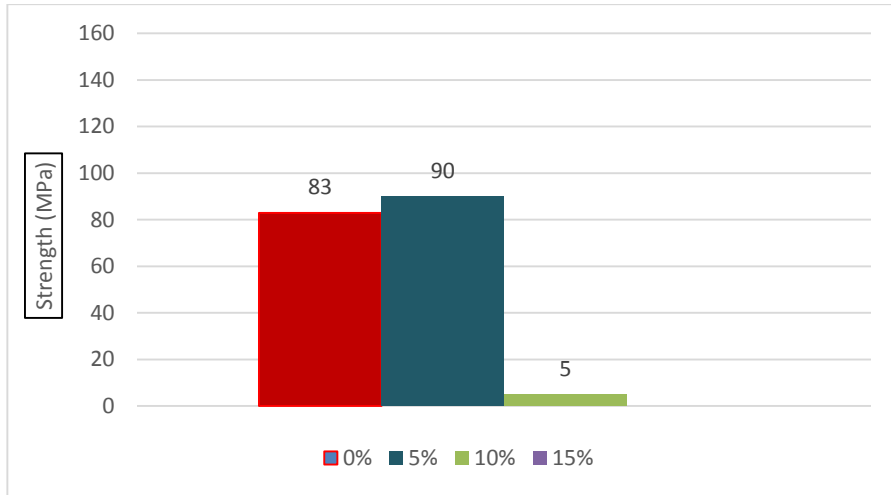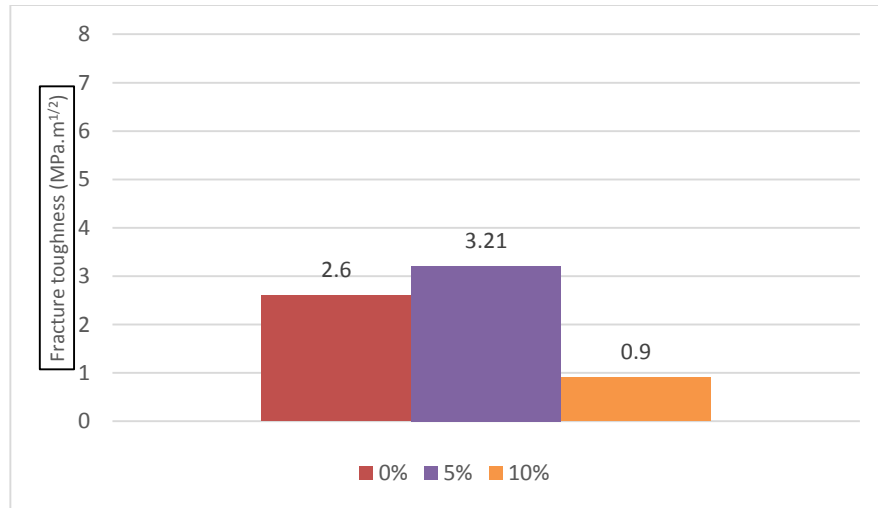
66

(a)

(b)

Figure 5.24 : (a) Flexural strength (b) Fracture toughness values of tetragonal stabilized zirconia with addition of TiO_2 sintered at 1600°C graph.

5.6 Monoclinic Zirconia With Addition of SiC

In the case of silicon carbide specimens, according to X-ray diffraction patterns and strength values sintering temperature was not enough high and specimens were not densificated.

Figure 5.25 illustates XRD patterns of SiC containing specimens. It is indicated that tetragonal and cubic is major phases in 0 wt% SiC sample, however, monoclinic phase was increased with increasing SiC content and led to reduce mechanical properties values.
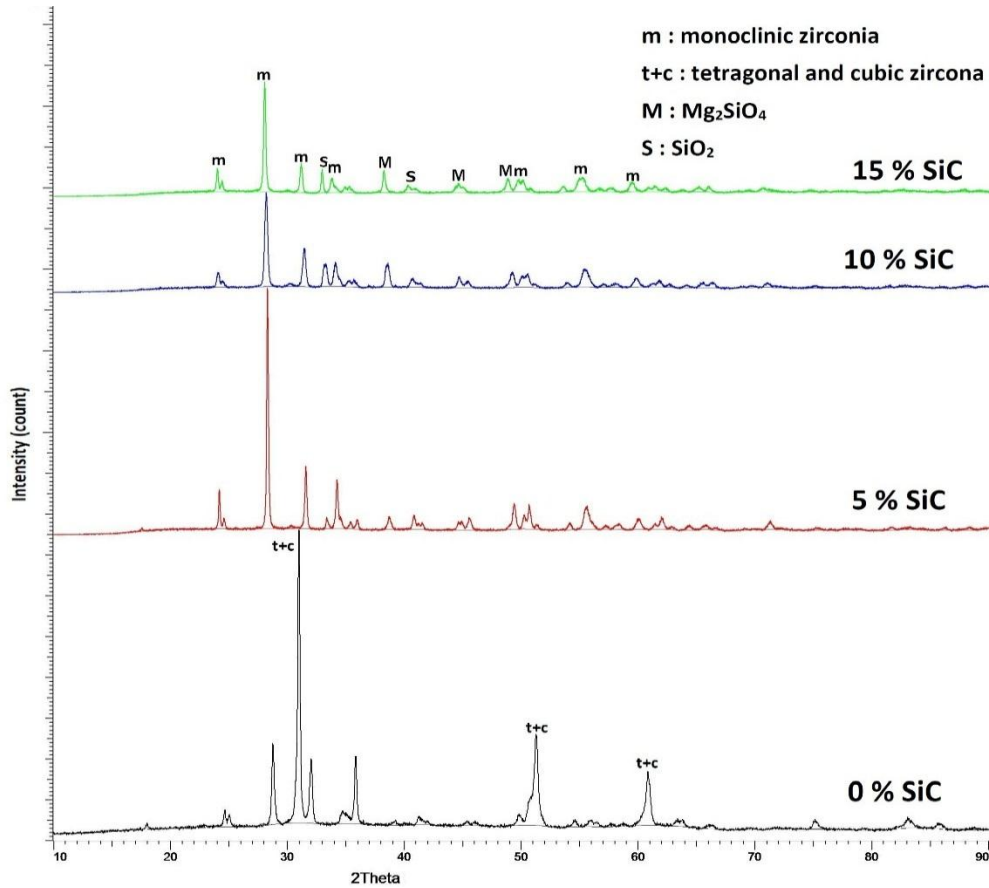
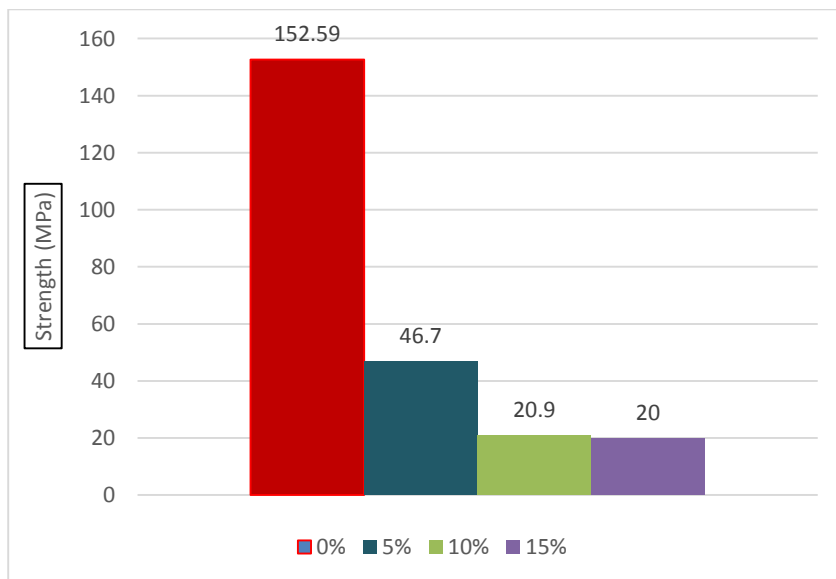**Figure 5.25 :** X-ray diffraction patterns of monoclinic zirconia with addition of SiC.

Figure 5.26 : Flexural strength values of zirconia with addition of SiC

6. CONCLUSIONS

a) Monoclinic zirconia with 3.12 wt% MgO as stabilizer, and 0, 5, 10 or 15 wt% Si_3N_4 have been sintered at 1600°C for 2 hours in nitrogen atmosphere.

- XRD results indicated:

    1) In ZrO_2 containing 5 wt% Si_3N_4 specimen, monoclinic phase was decreased and tetragonal, cubic and zirconium oxide nitride phase were formed (β:$Zr_7O_8N_4$).

    2) In ZrO_2 containing 10 and 15 wt% Si_3N_4, zirconium oxide nitride structure is major phase.

- Decreasing densification of silicon nitride containing samples can be related to low powder density of silicon nitride (3.44 g/cm^3). Porosity of 5 wt% Si_3N_4 is higher than other speciemens because of existing large amount of porosity in grain boundaries, which filled by liquid phase in high content of Si_3N_4.

- Flexural strength fracture toughness values are increased by increasing Si_3N_4 content.

- It can be seen that the hardness of the specimens decreased with increasing Si_3N_4 content up to 5 wt% and further increase led to an increase in hardness. The decrease of hardness in 5 wt% Si_3N_4 can be attributed to high amount of porosity. The highest hardness value is 14.2 GPa of 15 wt% Si_3N_4 amoung all samples.

b) Monoclinic zirconia with 3.12 wt% MgO as stabilizer, and 0, 5, 10 or 15 wt% TiO_2 have been sintered in two different processes : 1) at 1400°C for 2 hours, 2) at 1600°C for 5 hours then aged at 1100°C for 4 hours.

- XRD analysis revealed $Mg_2Zr_5O_{12}$ structure and tetragonal phase formed only in 5 wt% TiO_2 containing specimens sintered at 1400°C. Doping TiO_2 to zirconia was destabilized zirconia and reacted with MgO.

- Density of all samples decreased with increasing of TiO_2. This decreased density can be due to the grain growth and increasing amount of intergranular porosity.

- Sintering at higher temperature and ageing leads to formation needle-like tetragonal structure, however, increasing grain size was removed its effect.

- Hardness was reduced with increasing TiO_2 content, and it can be explained by increasing amount of porosities.

- Zirconia containing 5 wt % TiO_2 was showed relatively high flexural strength (115.6 Mpa) and fracture toughness (4.28 $MPa.m^{1/2}$).

c) Tetragonal stabilized zirconia with addition of 0, 5, 10 or 15 wt% TiO_2 have been sintered in two different processes : 1) at 1400°C for 2 hours, 2) at 1600°C for 5 hours then aged at 1100°C for 4 hours.

- XRD analysis revealed $Mg_2Zr_5O_{12}$ structure and tetragonal phase formed only in 5 wt% TiO_2 containing specimens in both two process. Doping TiO_2 to zirconia was destabilized zirconia and reacted with MgO.

- With increasing TiO_2 content, density of samples sintered at 1400°C increased because of slow grain growth, and density of samples sintered at 1600°C decreased.

- Sintering at higher temperature and ageing leads to formation needle like tetragonal structure, however, increasing grain size was removed its effect.

- Hardness was reduced with increasing TiO_2 content, and it can be explained by increasing amount of porosities.

- Zirconia containing 5 wt % TiO_2 was showed relatively high flexural strength (115.1 MPa) and fracture toughness (4.17 $MPa.m^{1/2}$).

- Doping TiO_2 and sintering at 1400°C without ageing process presented better mechanical properties for both monoclinic and tetragonal powder. Also increasing TiO_2 over 5 wt% changed microstructure, where decreased hardness, flexural strength and fracture toughness values.

REFERENCES

[1] **James, F., Robert, H.** (2008). Ceramic and glass materials: Structure, properties and processing. London: Springer.

[2] **Tekeli, S., Güral, A.** (2007). Sintering, phase stability and room temperature mechanical properties of c-ZrO$_2$ ceramics with TiO$_2$ addition. *Materials & design*;28,5. p: 1707-10.

[3] **Bocanegra-Bernal, M., De La Torre, S. D.** (2002). Phase transitions in zirconium dioxide and related materials for high performance engineering ceramics. *Journal of materials science*;37,23. p: 4947-71.

[4] **Stevens, R.** (1983). An Introduction to Zirconia, Magnesium Electron. *Publication No 113*.

[5] **Dorn, M., Nickel, K.** (2003). Zirconia ceramics: phase transitions and Raman microspectroscopy. *High Pressure Surface Science and Engineering*. p: 467.

[6] **Garvie, R., Hannink, R., Pascoe, R.** (1975). Ceramic steel?

[7] **Hannink, R. H., Kelly, P. M., Muddle, B. C.** (2000). Transformation toughening in zirconia-containing ceramics. *Journal of the American Ceramic Society*;83,3. p: 461-87.

[8] **Pilathadka, S., Vahalová, D., Vosáhlo, T.** (2007). The Zirconia: a new dental ceramic material. An overview. *Prague Med Rep*;108,1. p: 5-12.

[9] **Lughi, V., Sergo, V.** (2010). Low temperature degradation-aging-of zirconia: A critical review of the relevant aspects in dentistry. *Dental materials*;26,8. p: 807-20.

[10] **Heimann, R. B.** (2010). Classic and advanced ceramics: from fundamentals to applications: John Wiley & Sons.

[11] **Swab, J. J.** (2001). Role of Oxide Additives in Stabilizing Zirconia for Coating Applications. DTIC Document.

[12] **Kelly, J. R., Denry, I.** (2008). Stabilized zirconia as a structural ceramic: an overview. *Dental Materials*;24,3. p: 289-98.

[13] **Basu, B., Vleugels, J., Van Der Biest, O.** (2004). Transformation behaviour of tetragonal zirconia: role of dopant content and distribution. *Materials Science and Engineering: A*;366,2. p: 338-47.

[14] **Basu, B., Balani, K.** (2011). Advanced structural ceramics: John Wiley & Sons.

[15] **Riedel, R., Chen, I.-W.** (2011). Ceramics Science and Technology, Materials and Properties: John Wiley & Sons.

[16] **Schelling, P. K., Phillpot, S. R., Wolf, D.** (2001). Mechanism of the Cubic-to-Tetragonal Phase Transition in Zirconia and Yttria-Stabilized Zirconia by Molecular-Dynamics Simulation. *Journal of the American Ceramic Society*;84,7. p: 1609-19.

[17] **Mercera, P., Van Ommen, J., Doesburg, E., Burggraaf, A., Roes, J.** (1991). Stabilized tetragonal zirconium oxide as a support for catalysts Evolution of the texture and structure on calcination in static air. *Applied catalysis*;78,1. p: 79-96.

[18] **Fabris, S., Paxton, A. T., Finnis, M. W.** (2002). A stabilization mechanism of zirconia based on oxygen vacancies only. *Acta Materialia*;50,20. p: 5171-8.

[19] **Bechepeche, A., Treu Jr, O., Longo, E., Paiva-Santos, C., Varela, J. A.** (1999). Experimental and theoretical aspects of the stabilization of zirconia. *Journal of materials science*;34,11. p: 2751-6.

[20] **Xia, F., Zhang, H.** (2013). Effect of thermal treatment on microstructure and phase of partially-stabilized zirconia. *Journal of Wuhan University of Technology-Mater Sci Ed*;28,3. p: 483-6.

[21] **Gupta, T., Bechtold, J., Kuznicki, R., Cadoff, L., Rossing, B.** (1977). Stabilization of tetragonal phase in polycrystalline zirconia. *Journal of Materials Science*;12,12. p: 2421-6.

[22] **Jacobson, N. S.** (1989). Thermodynamic properties of some metal oxide-zirconia systems. DTIC Document.

[23] **Liu, Q., An, S., Qiu, W.** (1999). Study on thermal expansion and thermal shock resistance of MgO-PSZ. *Solid State Ionics*;121,1. p: 61-5.

[24] **Chevalier, J. m., Gremillard, L., Virkar, A. V., Clarke, D. R.** (2009). The tetragonal-monoclinic transformation in zirconia: lessons learned and future trends. *Journal of the American Ceramic Society*;92,9. p: 1901-20.

[25] **Piconi, C., Maccauro, G.** (1999). Zirconia as a ceramic biomaterial. *Biomaterials*;20,1. p: 1-25.

[26] **Refractories, M.** (1992). Handbook of Refractory Practice. Harbison-Walker Pittsburgh: Indresco inc.

[27] **Schacht, C.** (2004). Refractories handbook: CRC Press.

[28] **Cirilli, F., Di Donato, A., Martini, U., Miceli, P., Guillo, P., Simoes, J., et al.** (2008). CORROSION MECHANISMS OF ZIRCONIA/CARBON BASED REFRACTORY MATERIALS BY SLAG IN PRESENCE OF STEEL. *la metallurgia italiana*10.

[29] **Url-1**<http://www.ifglref.com/product_pdf/tundish_metering_nozzles.pdf>, date: 11.04.2015.

[30] **Url-2**<http://www.zircoa.com/product.related/overview.html>, date: 11.04.2015.

CURRICULUM VITAE

Name Surname: Sina Sadigh Akbari

Place and Date of Birth: 30.03.1990, Tabriz, Iran

E-Mail: ssadighakbari@gmail.com

EDUCATION:

B.Sc.: 2008-2013, University of Tabriz, Materials Engineering.

M.Sc.: 2013-2015, Istanbul Technical University, Materials Engineering.

PROFESSIONAL EXPERIENCE AND REWARDS:

PUBLICATIONS, PRESENTATIONS AND PATENTS ON THE THESIS:

Submitted "Mechanical properties of partially stabilized zirconia with addition of Si_3N_4" The Eleventh Conference for Young Scientists in Ceramics (SM-Serbia 2015).

OTHER PUBLICATIONS, PRESENTATIONS AND PATENTS :